九州大学学術情報リポジトリ
Kyushu University Institutional Repository

Comparative study of age-associated epigenetic modifications using human cohorts and mouse models

岩谷, 千寿

https://doi.org/10.15017/1931734

出版情報：九州大学, 2017, 博士（理学）, 課程博士
バージョン：
権利関係：

KYUSHU UNIVERSITY

Comparative study of age-associated epigenetic modifications using human cohorts and mouse models

Chihiro Iwaya

Graduate School of Systems Life Sciences, Kyushu University

Contents

Abbreviations

GWAS: Genome-wide association study

EWAS: Epigenome-wide association study

PBC: Peripheral blood cell

T2D: Type 2 diabetes mellitus

TSS: Transcription starting site

MC: Methylation changes

ELOVL2: Elongation of very long chain fatty acids protein 2

FHL2: Four and a half LIM domain 2

TRIM59: Tripartite motif containing 59

KLF14: Krüppel-like factor 14

GLM: Generalized liner model

FACS: Flow cytometry

CBA: Cytometric Bead Array

SVF: Stromal vascular fraction

IFN-γ: Interferon-γ

IL-12: Interleukin-12

IL-1β: Interleukin-1β

IL-6: Interleukin-6

TNF-α: Tumor necrosis factor-α

SD: standard error

Abstract

Epigenetic modifications such as DNA methylation and histone modification play critical roles in many physiological processes such as the maintenance of homeostasis, adaptation to the environment and disease development. Using an epigenome-wide association study, I identified 22 CpG sites located in 17 loci that showed significant age-related methylation, including genes known to be associated with common adult-onset diseases such as *ELOVL2*, *FHL2 TRIM59* and *KLF14*. I then examined the methylation levels of CpG sites in the mouse counterparts *Elovl2*, *Fhl2*, *Trim59* and *Klf14* using various mouse organs of different ages. Among the four genes, *Elovl2* and *Klf14* replicated significant age-related methylation changes in mice with different organ specificities. The age-related epigenetic change in *Elovl2* was observed only in the colon, spleen, lung and tail, while the age-related epigenetic change in *Klf14* was observed only in the kidney, lung, spleen, colon, adipose tissue and peripheral blood cells (PBCs). *Fhl2* and *Trim59* failed to replicate significant epigenetic differences in mice. I also observed significantly decreased gene expression of *Klf14* in adipose tissue and PBCs correlated with the increased methylation level in *Klf14*, but not in *Elovl2*. As *KLF14* is known to be associated with T2D, I examined the possibility of *KLF14*/*Klf14* as an epigenetic biomarker of T2D by comparing the expression levels and methylation levels in T2D model mice (*db*/*db*) and obese mice treated with a high-fat diet (HFD). I observed a significant increase in methylation levels in *Klf14* in the spleen, adipose tissue and PBCs in T2D and obese mice. I also observed a significant decrease in the expression levels of multiple downstream genes regulated by *Klf14* in the adipose tissue in T2D and obese mice. By contrast, the expression levels of two inflammatory genes, *Il-12* and *Tnf*-α, were significantly increased in obese mice. By FACS analysis, I confirmed that the inflammatory mediators IFNγ, IL-6 and IL-1β as well as TNF-α and IL-12 shared significant increases in obese mice, yet IL-12 and TNF-α were the most responsive cytokines to obesity, demonstrating a 7-fold and 3-fold increase, respectively. Finally, I observed that the increased methylation levels in HFD-fed mice could be reversed by switching back to a normal-food diet (NFD), possibly correlated with weight loss. These results suggest that methylation changes in *KLF14* may also be associated with changes in gene

expression and inflammation status in human adipose tissue with obesity and/or T2D. In addition, the detectable methylation changes in *KLF14* in PBCs at the subclinical stage may serve as a predictive epigenetic biomarker for the development of T2D.

Introduction

Epigenetics is a term denoting hereditary changes in gene expression without changes in the DNA sequence. Many recent papers have reported critical roles of epigenetic changes in many biological processes, such as tissue differentiation, maintenance of homeostasis and adaptation to the environment [*e.g.*, Bernstein et al. (2007); Gut et al. (2013); Trerotola et al. (2015)]. Two major mechanisms of epigenetic modifications are DNA methylation and histone modification. Both affect the local chromatin structure and eventually regulate the gene expression level. In addition to their biological relevance, epigenetic modifications are significantly associated with some physiological states such as chronological age, obesity and disease [Richardson (2003); Rakyan et al. (2011)]. These findings hold substantial promise for identifying mechanisms through which genetic and environmental factors contribute to risks for human diseases [Civelek and Lusis (2014)]. It is well known that aging is associated with an increased risk for many diseases, including dementia, cardiovascular diseases, inflammatory diseases, metabolic diseases, age-related macular degeneration and cancer. DNA methylation levels in specific sites are known to change depending on chronological age [Garagnani et al. (2012); Hannum et al. (2013); Rönn et al. (2015)], suggesting that age-associated epigenetic change resulting in changes in gene expression is one of the molecular mechanisms accounting for the risk for multifactorial diseases.

The prevalence of diabetes is globally increasing and reached 425 million adults worldwide in 2017 (www.idf.org/diabetesatlas). Type 2 diabetes, T2D, is a long-term metabolic disorder characterized by hyperglycemia and insulin resistance. Complications due to hyperglycemia and insulin resistance include heart disease, stroke, and diabetic retinopathy. The factors contributing to the incidence of T2D are not only genetic background but also physiological status such as chronological age, obesity and little exercise, which is why it is called a lifestyle disease. Genome-wide association studies (GWASs) have identified more than 100 independent SNPs that are significantly associated with T2D [Manolio et al. (2009); Imamura and Maeda (2011); Morris et al. (2012); Flannick et al. (2016)]. However, the

whole picture of T2D has not yet been solved because, in addition to the additive effects of multiple susceptible genes, acquired but partially heritable modifications such as epigenetic changes play important roles in the onset of T2D as the “missing heritability” component [Ling et al. (2009); Manolio et al. (2009); Trerotola et al. (2015)].

In this study, I examined the association of DNA methylation with chronological age in human and mouse models. I also examined the association of DNA methylation with T2D and obesity in mouse models. In the first part of the study, I report the results of EWAS using 480 general Japanese subjects of different ages, in whom I identified 22 CpG sites located in 17 loci showing statistically significant methylation changes associated with age. Among the significant genes with age-associated methylation, I focused on *ELOVL2*, *FHL2*, *TRIM59* and *KLF14* since these genes have been reported to be associated with age-related diseases in other GWASs. In subsequent parts of this study, I investigated methylation changes in the promoter regions of the mouse counterparts *Elovl2*, *Klf14* and *Fhl2* in various organs in C57BL/6J (B6) mice of different ages. I also examined the methylation changes in *Klf14* during different physiological states such as T2D and obesity caused by a high fat diet (HFD) using C57BLKS/J Iar -＋Lepr^{db} /+Lepr^{db} (*db/db*) as T2D model mice and B6 mice. I examined the age-related methylation status in *Elovl2* and *Klf14* in different organs. I also examined the correlation of the methylation status of *Klf14* with gene expression levels of *Klf14* as well as downstream genes, and with the inflammatory status in adipose tissue. Finally, I discuss the potential use of *KLF14* as a biomarker for obesity and T2D.

Materials and Methods

Human subjects

The 288 subjects in the Fukuoka Cohort Study were selected from the participants in the baseline survey of the Kyushu University Fukuoka Cohort Study, which is an ongoing general population-based cohort. They were 50- to 75-year-old residents of the East Ward in Fukuoka City, and they participated in the survey from February 2004 to August 2007 and provided informed consent for genetic analysis. Details of the study are available elsewhere [Nanri et al. (2008); Ohnaka et al. (2009)]. The 192 subjects were selected from the participants in the KING (KItaNagoya Genome) Study, who were 55 to 82-year-old males undergoing community-based annual health checkups in Kitanagoya City. Male subjects without diabetes mellitus were chosen because they were also used as part of the control subjects in an epigenome-wide association study of coronary artery disease (Supplementary Table 1). Non-diabetic subjects were defined as having a fasting plasma glucose concentration < 7.0 mmol/L, a hemoglobin A1c level (measured according to the Japan Diabetes Society method) < 6.5%, or no current treatment for diabetes in the baseline data. Details of the study are available elsewhere [Asano et al. (2010)]. Informed consent in accordance with the Declaration of Helsinki was acquired from all subjects. The Ethics Committee at Kyushu University, Fukuoka, Japan, also approved this study.

Epigenome-wide association study (EWAS).

Bisulfite treatment was applied to genomic DNA extracted from PBCs using the EZ-96 DNA Methylation Kit (Zymo Research), which induces both bisulfite conversion and DNA cleanup in a 96-well plate. Genome-wide DNA methylation profiles were acquired by the Illumina HumanMethylation450 BeadChip (Illumina) according to the manufacturer's instructions. GenomeStudio V2011.1 (methylation module version 1.9.0) was used to calculate the beta values indicative of the estimated methylation level of each CpG site. The beta value was defined as follows: Max (signal for methylation, 0) / [Max (signal for methylation, 0) + Max (signal for unmethylation, 0) +

100]. Using this metric, the DNA methylation level was expressed by a number between 0 (no methylation) and 1 (complete methylation). The signal intensities were normalized to internal controls and background before beta value calculation.

To exclude outliers, principal component analysis (PCA) was performed for each of the four sample sets (96 samples in each set) using a total of 473,864 CpG sites on autosomes. One subject was detected as an outlier in the Fukuoka Cohort Study and eliminated from further analyses. Then, 273 and 3,163 CpG sites in the Fukuoka Cohort Study and KING Study, respectively, showing a call rate < 0.95, were excluded from the statistical analyses. The call rate of all samples was > 0.99.

I analyzed the association between the DNA methylation level of autosomes and age using a generalized linear regression model (GLM) adjusting for sex and body mass index (BMI) in the Fukuoka Cohort Study set and adjusting for BMI in the KING Study set [Michels et al. (2013)]. I selected common age-associated DNA methylation levels that passed the conservative Bonferroni corrected significance level ($P < 1.05 \times 10^{-7}$ accounting for 473,864 tests) in both sets and combined the two sets to perform further analyses. I affirmed that the selected age-associated DNA methylation sites also passed the conservative Bonferroni corrected significance level in the combined set using GLM by adjusting for sex and BMI. I defined the most significant site in each locus as the representative age-associated DNA methylation site (landmark site) and used the 17 landmark sites for further analyses (Supplementary Fig. 1).

I used R version 2.14.2 for GLM. The information for the genes, methylation sites loci, SNPs, and GWAS catalog were based on the database of NCBI37/hg19 [Kent et al. (2002); Karolchik et al. (2004)].

Mouse subjects

All mouse work was conducted according to the relevant national and international guidelines. C57BL/6J (B6), BALB/cByj (Balb), C57BLKS/J Iar -+Lepr^{db} /+Lepr^{db} (*db*/*db*), and C57BLKS/J Iar -m+/+Lepr^{db} (+/*db*) were purchased from CLEA Japan Inc. (Tokyo, Japan). All mice were bred under

pathogen-free conditions with free access to water and food at the Center of Biomedical Research, Research Center for Human Disease Modeling, Graduate School of Medical Sciences, Kyushu University, Fukuoka, Japan. The ethics committees of Kyushu University approved all experimental protocols. All diet foods were purchased from Oriental Yeast. A schematic diagram of the mouse treatments is shown in Supplementary Fig. 2. To examine age-related epigenetic changes, I prepared "Young" and "Aged" B6 (Supplementary Fig. 2A) and Balb mice (Supplementary Fig. 2B) following the treatment. I dissected 4- and 50-week-old mice as the "Young and "Aged" groups, respectively. I prepared 5 male and 5 female diet-matched mice for each treatment. To examine the T2D-related epigenetic changes, I prepared age-, sex- and diet-matched "T2D" and "Healthy" groups following the treatment shown in Supplementary Fig. 2C. I used 12-week-old homozygous *db*/*db* mice and heterozygous +/*db* mice as the "T2D" and "Healthy" groups, respectively. To examine obesity-related epigenetic changes, I prepared age- and sex-matched "Normal" and "Obese" groups following the treatment shown in Supplementary Fig. 2D. I raised male B6 mice (n = 50) for 4 weeks only with the normal food diet (NFD; 11.5% from fat), and then switched to the high fat diet (HFD; 62.2% from fat) only 25 mice as the "Obese" group while continuing to raise the remaining 25 mice with NFD as the "Non-obese" group. I sacrificed 5 mice from each treatment every week to collect 4, 5, 6, 7 and 8-week-old mice on two different diets. To examine diet-related epigenetic changes, I treated age-, sex-matched mice with three different dietary conditions as shown in Supplementary Fig. 2E. I raised 20 male B6 mice with only NFD for 16 weeks as the "N-only" (NFD-only) group. I also raised another 20 male B6 mice with NFD for 4 weeks and then switched them to HFD for 12 weeks as the "N-H" (NFD-HFD) group. In addition, I raised another 20 male B6 mice with NFD for 4 weeks, then switched them to HFD for 4 weeks and further them switched back to NFD for 8 weeks as the "N-H-N" (NFD-HFD-NFD) group. I sacrificed 5 mice each per treatment every 4 weeks to collect 4, 8, 12, and 16-week-old mice receiving three different dietary conditions. After dissection of the samples, I collected the cerebrum, cerebellum, heart, lung, liver, pancreas, spleen, colon, kidney, testis (or the ovary), adipose tissue (epididymal white adipose tissue), tail tissue and PBCs (Supplementary Table 2).

Intra peritoneal glucose tolerance test (IPGTT)

Peripheral blood samples were obtained from the tail vein. Plasma glucose concentrations were determined based on plasma insulin concentrations by ELISA (Morinaga Institute of Biological Science). After a 16-h fast, glucose tolerance was assessed by an Intra-peritoneal glucose tolerance test (IPGTT). Briefly, under anesthesia with 2% (vol./vol.) isoflurane via facemask for 1.5 min, a glucose bolus (1 g / kg i.p.) was injected, and peripheral blood samples were collected from the tail vein at 0, 15, 30, 60, 90 and 120 min.

Extraction of genomic DNA and RNA

I extracted genomic DNA from ≤ 25 mg of frozen tissue (≤ 10 mg of the spleen) using PureLink® Genomic DNA (Invitrogen). Total RNA was extracted from ≤ 30 mg of the frozen organs (≤ 10 mg of the spleen) using the RNeasy Plus Mini Kit (QIAGEN). The experiments were performed according to the manufacturer's instructions. DNA and RNA concentrations were measured with a NanoDrop photometer (SCRUM Inc.).

Bisulfite pyrosequencing

Genomic DNA was treated with bisulfite using the EZ-96 DNA Methylation Kit (Zymo Research) according to the manufacturer's instructions. The bisulfite-treated DNA was then amplified by PCR using the following primer pair: Forward 5'-GGTAGGGTTGGGATTTGTAAGTAT-3' and Reverse 5' biotin-CCCCTCAAACCCCTATACCC- -AATTTA-3' with the following conditions: 40 cycles of 96°C for 30 s, 55°C for 30 s and 72°C for 30 s, without a final extension. For each PCR, 12.5 mM $MgCl_2$, 15 μM dNTP Mixture, 20 pmol forward and reverse primers, 1.25 U of TaKaRa EpiTaq HS (TaKaRa), 5 μl of 10×EpiTaq PCR buffer (TaKaRa) and 100 ng of the bisulfite-treated DNA were used in a 50 μl total reaction volume. After PCR, the quality was evaluated by 1% agarose gel electrophoresis, allowing the identification of the product size. The PCR products were subsequently pyrosequenced by ALLIANCE Biosystems. The DNA methylation status was evaluated and visualized using R (version

2.15.0). The difference in methylation levels among organs was evaluated by t-tests. For individual tests, I set the level of significance at 0.05. For multiple testing, the corrected *P* value (*Pc*) was obtained by the Bonferroni method by multiplying the raw *P* values by the number of organs tested ($n = 11$).

Bisulfite sequencing by cloning.

Genomic DNA was treated with bisulfite using the EZ DNA Methylation Kit (Zymo Research) according to the manufacturer's instructions. The bisulfite-treated DNA was then amplified by PCR using the following primer pairs: *Elovl2* Forward 5'-GGTAGGGTTGGGATTTGTAAGTAT-3' and Reverse 5'-CCCCTCAAACCCCTATACCCAATTTA-3'; *Fhl2* Forward 5'-TTTTTGTGTTTTAAGTAGGGTTGTG-3' and Reverse 5'-AATAACAATAACCCCATATCATTTC-3'; *Trim59* Forward 5'-GTTTTGGGGGGGAAGGGT-3' and Reverse 5'-ACCCTCCAACCCATAACTAAACAAAAAAC-3'; *Klf14* Forward 5'-ATGGTATTTTTAGTAGTTTGGGAAATTA-3' and Reverse 5'-TAAAACTCTACCTAACACCCAACTA-3'. For each PCR, TaKaRa EpiTaq HS (TaKaRa) was used. Amplified DNA was cloned using the TOPO TA Cloning Kit (Invitrogen) and pGEM T Easy Vector System1 (Promega). The insert was amplified by PCR using standard vector-specific M13 forward and reverse primers under the following condition: 30 cycles of 96°C for 30 s, 55°C for 30 s, and 72°C for 30 s, with a final extension at 72°C for 5 min. The sequence data were obtained from approximately 36-48 clones for each sample using the 3730 DNA Analyzer (Applied Biosystems). The sequences of the target sites for *Elovl2*, *Fhl2*, *Trim59* and *Klf14* are depicted in Figures 2 and 3 and Supplementary Figure 3A and B, respectively. The mean value of 5 mice was subjected to statistical analysis to calculate each MC.

Quantitative reverse transcription PCR

Reverse transcription reaction was performed using a High Capacity cDNA Reverse Transcription Kit (Applied Biosystems). cDNA was prepared from 1 μg of total RNA with random hexamer primers according to the manufacturer's instructions. The analysis of *Elovl2* expression was performed using TaqMan probes Mm00517086_m1 for *Elovl2* (Applied Biosystems) and Mm99999915-g1 for mouse *Gapdh* (Applied Biosystems). All amplifications were carried out in triplicate. The 7900HT Sequence Detection System (Applied Biosystems) was employed for data collection. Comparative analyses of *Elovl2* and *Gapdh* were performed using the specialized computer program SDS 2.2.2 (Applied Biosystems). The mRNA expression level of *Elovl2* was calculated by the $2^{-\Delta\Delta CT}$ (relative quantity) method according to the instructions provided in the manual supplied with the TaqMan® Low Density Array (Applied Biosystems).

For *Klf14* and the downstream genes, mRNA levels were quantified by quantitative reverse transcription PCR using Go Taq qPCR Master Mix (Promega) with the LightCycler 480 System II (Roche). The primers used for each target gene are summarized in Supplementary Table 3. The linearity of the amplification as a function of the cycle number was tested in preliminary experiments, and mRNA expression levels were normalized to the expression level of β-actin. The mRNA expression levels of *Klf14* were calculated by the $2^{-\Delta\Delta CT}$ (relative quantity) method.

Cytokine Analysis

Concentrations of five different antigenic factors were determined in both serum and SVF samples using the BDTM Mouse CBA Enhanced Sensitivity Flex Set (BD Pharmingen) with mouse IL-6 (BD Pharmingen, #562236), mouse IL-12 (BD Pharmingen, #562264), mouse TNF-α (BD Pharmingen, #562336), mouse IL-1β (BD Pharmingen, #562278), and mouse IFN-γ (BD Pharmingen, #562233) [Morgan et al. (2004)]. Each CBA Set contained one bead population with a distinct fluorescence intensity as well as the appropriate phycoerythrin (PE) detection reagent and standard. Five bead populations coated with capture antibodies specific to IL-6, IL-12, TNF-α, IL-1β, and IFN-γ were

mixed with each other. The tests were performed according to the manufacturer's recommendations, and samples were run in duplicate. After addition of PE-conjugated detection antibodies, the samples were incubated again and then resolved in a FACS Verse flow cytometer (BD Pharmingen). The results were generated in graphic and tabular format using the CBA analysis software (BD Pharmingen).

Isolation of the stromal vascular fraction from adipose tissue

I removed the epididymis white adipose tissue and then minced it into small pieces. I incubated them at 37°C for 50 min in collagenase solution (2 mg/ml) of collagenase type A (Roche) in HEPES (Life Technologies) with gentle stirring. We then centrifuged 500 g of the digested tissue for 10 min, suspended the pellet containing the stromal vascular fraction into HEPES and filtered it through a 70-μm mesh. We washed the cells twice with HEPES and finally re-suspended them in cell staining buffer.

Statistical analysis for mouse study.

Statistical analysis was performed using the Student's t test and ANOVA followed by the Schaffer test. Data were expressed as the mean ± SD. P values < 0.05 were considered statistically significant.

Chapter 1: Epigenome-wide association study (EWAS) with age

To identify age-associated changes in DNA methylation levels, I analyzed two sample sets from ongoing general population cohort studies: 288 samples from the Fukuoka Cohort Study and 192 samples from the KING Study. DNA methylation levels were obtained using the Illumina Human Methylation 450K BeadChip, and the data for 473,864 autosomal DNA methylation sites were analyzed using a GLM with adjustment for gender and BMI in each sample set (Supplementary Fig. 1 and Supplementary Table 1). I found that both sample sets shared the identical 22 age-associated DNA methylation sites in the same direction and thus reached the conservative Bonferroni threshold ($P < 1.05 \times 10^{-7}$ accounting for 473,864 tests, Table 1). The 22 sites corresponded to 17 loci including 15 genic regions of the following genes: *CC2D2A*, *TRIM2*, *SERINC5*, *KLH35*, *C1R*, *RASSF5*, *MIR29B2*, *FHL2*, *SFMNT1*, *TRIM59*, *PCDHB1*, *ELOVL2*, *NHLRC1*, *KLF14* and *OTUD7A*. Scatter plots of representative methylation sites of the 17 loci showed a nearly linear change in the DNA methylation level with aging (Fig. 1). Among the 22 age-associated CpG sites, the 15 sites (10 loci) presented higher DNA methylation levels with advancing age, and the other seven sites (seven loci) showed lower DNA methylation levels.

The most significant age-associated DNA methylation site was cg16867657 located near the 5' end of *ELOVL2* ($P = 1.7 \times 10^{-45}$, Table 1). *ELOVL2* also harbors two additional significant CpG sites, cg21572722 and cg24724428 with the ninth and the eleventh lowest *P* values (2.0×10^{-37} and 5.3×10^{-31}, respectively, in Table 1). *ELOVL2* is known to contribute to the long-chain polyunsaturated fatty acid (PUFA) metabolic pathway [Leonard et al. (2002); Ohno et al. (2010)]. The second, third, and fourth lowest *P* values were found in cg06639320, cg22454769, and cg24079702 ($P = 2.8 \times 10^{-40}$, 2.0×10^{-37}, and 5.3×10^{-31}, respectively, Table 1) located near the 5' end of *FHL2*, which is known to be associated with osteoporosis [Günther et al. (2005); Johannessen et al. (2006)]. The fifth lowest *P* value ($P = 3.6 \times 10^{-28}$, Table 1) was found in cg07553761 near the 5' end of *TRIM59*, which is known to be associated with the tumorigenesis of various cancers including lung cancer and stomach cancer [Khatamianfar et al. (2012); Zhou et al. (2014)]. The sixth lowest *P* value ($P = 6.7 \times 10^{-26}$, Table 1) was

found in cg04875128 located near the 3' end of *OTUD7A*, which has been reported to be associated with neurodevelopmental phenotypes [Shinawi et al. (2009)]. The seventh lowest *P* value ($P = 2.3 \times 10^{-25}$, Table 1) was found in cg08097417 located near the 5' end of *KLF14*, which also harbors another significant site, cg14361627, with the 15th lowest *P* value (1.6×10^{-19}, Table 1). *KLF14* has been reported to be associated with T2D and with serum levels of HDL-cholesterol [Manolio et al. (2008); Teslovich et al. (2010); Imamura and Maeda (2011); Morris et al. (2012); Flannick and Florez (2016)]. The tenth lowest *P* value ($P = 2.3 \times 10^{-22}$, Table 1) was found for cg22736354 in an exon region of *NHLRC1*, which is known to be associated with progressive myoclonus epilepsy [Chan et al. (2003); Singh et al. (2009)].

Chapter 2: Conservation of age-associated CpG sites between human and mouse

Based on the EWAS result, I selected four genes of those genetic variations were known to be associated with multifactorial diseases, namely, *ELOVL2*, *FHL2*, *TRIM59* and *KLF14,* for further studies using mouse models. These CpG sites have been reported to be associated with age in previous EWASs from different ethnic groups [Berdasco and Esteller (2012); Garagnani et al. (2012); Rönn et al. (2015)]. I investigated whether genome sequences in which age-associated CpG sites were originally identified in humans were conserved in mice.

As shown in Fig. 2, the most significant CpG site, namely, cg16867657, was not a conserved cytosine. Consequently, I analyzed cg24724428, which is located at -264 bp from the transcription starting site (TSS) of *ELOVL2*. The BLAST search using the genome sequence around cg24724428 revealed the highly conserved sequence in the promoter region of mouse *Elovl2*. The 49 bases from -240 to -285 of *ELOVL2* showed 41.3% identity to the sequence from -291 to -339 of *Elovl2* (Fig. 2). It is noted that the cg24724428 CpG site was conserved between human and mouse (Fig. 2). This conservation indicates that this genomic region in mice is appropriate for a proxy target for further DNA methylation analyses of human *ELOVL2*. The predicted nucleotide sequence of the region of *Elovl2* after bisulfite treatment is also shown at the bottom of Fig. 2. I designed PCR primers

(highlighted by a shadow) and a sequence primer (underlined) for pyrosequencing to determine the methylation levels of four CpG sites: P1-P4, where the P4 corresponds to the mouse-cg24724428 site.

Like cg16867657, the second significant CpG site, cg06639320, was also not conserved. I examined the next significant site, cg22454769, located -196 bp from the TSS of *FHL2*. The BLAST search using the genome sequence around cg22454769 revealed the conserved sequence in the intronic region of mouse *Fhl2* (Supplementary Fig. 3A). Although it was not a promoter region, a primer was designed around the conserved region (Supplementary Fig. 3A). The 49 bases from -58 to -106 of *FHL2* showed 28.6% identity to the sequence from +501 to +549 of *Fhl2* (Supplementary Fig. 3A).

The next significant CpG site, cg07553761, was located -351 bp from the TSS of *TRIM59*. The BLAST search using the genome sequence around cg07553761 revealed the conserved sequence in the promoter region of mouse *Trim59* (-206 bp upstream from the TSS). The 45 bases from -329 to -373 of *TRIM59* showed 55.6% identity to the sequence from -185 to -228 of Trim59 (Supplementary Fig. 3B).

The significant CpG site, cg14361627, was the only site with a conserved cytosine between human and mouse. In addition, it was located -228 bp from the TSS of *KLF14*. The BLAST search using the genome sequence around cg14361627 revealed the highly conserved sequence in the promoter region of mouse *Klf14*. The 46 bases from -206 to -250 of *KLF14* showed 81.8% identity to the sequence from -1 to -044 of *Klf14* (Fig. 3). It is noted that the cg14361627 CpG site was conserved between human and mouse (Fig. 3). This observation indicated that this genomic region in mice was appropriate for a proxy target for further DNA methylation analyses in human *KLF14*. The predicted nucleotide sequence of the region of *Klf14* after bisulfite treatment is also shown at the bottom of Fig. 3. There were 9 CpG sites: P1-P9 (Fig. 3). P3 is the CpG site that has been reported to be associated with age in previous EWASs [Berdasco and Esteller (2012); Garagnani et al. (2012); Rönn et al. (2015)]. I designed PCR primers (highlighted by a shadow) to determine the methylation levels of four CpG sites, P1-P9, where P3 corresponds to the mouse-cg14361627 site.

First, I examined age-related changes in the methylation level at the nine CpG sites (P1-P9) in *Fhl2* and *Trim59* (Supplementary Figure 4A and Supplementary Figure 5A) by bisulfite sequencing

with cloning using the DNA sampled from 11 different organs (Supplementary Figure 4B and Supplementary Figure 5B). Both genes failed to replicate the age-associated change I observed in human cohorts. Therefore, I did not pursue the examination of *Fhl2* and *Trim59* in the following studies.

Next, I examined the methylation levels of the CpG sites in *Elovl2* by pyrosequencing using DNA samples prepared from 12 organs (cerebrum, cerebellum, heart, lung, liver, pancreas, spleen, colon, kidney, testis, ovary and tail) of 15 mice each from the "Young" and "Aged" groups (Fig. 1A). The methylation levels at the P3 site in the promoter region of *Elovl2* are shown as boxplots in Fig. 4A. I observed a statistically significant increase in methylation levels in the "Aged" mice in the lung (methylation change = 8%, *Pc* = 1.7E-07), spleen (MC = 12%, *Pc* = 1.4E-09), colon (MC = 28%, *Pc* = 4.3E-08) and tail (MC = 6%, *Pc* = 0.0001).

I then compared the methylation levels at the P1-P4 sites between "Young" and "Aged" mice in the colon and spleen. The methylation levels varied among the 4 sites in both the "Young" and "Aged" groups (Fig. 4B). However, the order of the methylation levels of P3 > P2 > P1 ≥ P4 was conserved in the "Young" and "Aged" mice and conserved in the colon and spleen. This trend of methylation changes was also observed in other organs (Supplementary Fig. 6), suggesting that the methylation levels of these 4 sites are tightly linked under different physiological conditions.

One may argue that the age-associated methylation changes in *Elovl2* specifically observed in the lung, spleen, colon and tail could be different between sexes and/or between mouse strains. To clarify these issues, we examined the methylation levels at P3 in male and female B6 mice and in male Balb mice. Similar organ specificity and directions of methylation change with age were observed in both sexes and in both mouse strains (Supplementary Figs. 7 and 8). Taken together, the results strongly suggested that the age-associated DNA methylation increase in the *ELOVL2* promoter region originally identified in human PBCs was conserved in mouse. In addition, the epigenetic changes in *ELOVL2* might not only occur in PBCs but also in lung, spleen and colon in humans.

To obtain methylation data for the 5' additional sites located 3' downstream from P1-P4, we

performed bisulfite cloning-sequencing using the same PCR primer sets as applied for bisulfite pyrosequencing. A total of 48 clones generated from DNA prepared from colons obtained from the "Young" and "Aged" mice were selected and subjected to DNA sequence analysis. In addition to the P1-P4 sites, the P5-P9 sites also showed increased methylation levels in the "Aged" mice compared with the "Young" mice (Fig. 4C). The methylation changes did not occur in a position-specific manner; alteration of the methylation status was linked between the CpG sites of P1-P9. Therefore, we assumed that methylation might occur in *cis* and spread around the promoter region of *Elovl2*.

Next, I examined age-related changes in the methylation level at the nine CpG sites (P1-P9) in *Klf14* (Fig. 3) by bisulfite sequencing with cloning using the DNA sampled from the PBCs (Fig. 5A). In male mice, I observed an age-related increase in methylation levels at the six CpG sites, P1- P6, as also observed in humans. The most significant increase was observed in P3, the CpG site originally identified in my EWAS (MC = 35%, $P = 0.0008$). However, three sites, P6-8, did not show age-related methylation, suggesting that methylation might be transmitted in *cis* in the promoter region of *Klf14*. I also examined the methylation levels in the 9 CpG sites in the adipose tissue of the spleen in both sexes. I observed an age-related increase in the methylation level at nearly all the sites, with P3 consistently showing the largest fold-change (Supplementary Fig. 9).

I then examined age-related methylation at P3 in 11 organs (cerebrum, heart, lung, liver, pancreas, spleen, colon, kidney, testis (or the ovary), adipose tissue and PBCs). I observed a significant age-related increase in the methylation level in 7 organs: lung (MC = 18.3%, $P = 0.009$), spleen (MC = 38.3%, $P = 0.0007$), kidney (MC = 12.5%, $P = 0.0007$), colon (MC = 50.8%, $P = 0.006$), adipose tissue (MC = 42.5%, $P = 6.3E-05$), testis (MC = 31.7%, $P = 0.0005$) and PBCs (MC = 35%, $P = 0.0008$) (Fig. 5B). The increase in methylation levels was more pronounced in female mice (Supplementary Fig. 10). I detected similar patterns of position effects and organ specificities in female groups (Supplementary Fig. 10). It is notable that this result is consistent with the findings of human cohort studies [Berdasco and Esteller (2012); Garagnani et al. (2012); Rönn et al. (2015)]. The most responsive CpG site in all tested organs, including in females, was P3 (Supplementary Figs. 9 and 10).

I also compared the methylation level at P3 in *Klf14* using the DNA sampled from the spleen, adipose tissue and PBCs between age-, sex- and diet-matched "T2D" mice (*db*/*db*) [Srinivasan and Ramarao (2007)] and "Healthy" mice (+/*db*). I observed a significant increase in the methylation level in "T2D" mice compared with the healthy control (Fig. 5C and Supplementary Fig. 11). This result supported the methylation level of *Klf14* as a biomarker for T2D. If the methylation level of *Klf14* changes under the subclinical conditions of T2D, *Klf14* could be a promising epigenetic biomarker for T2D. Therefore, I compared the methylation levels at P3 between the "Obese" mice treated with HFD as a subclinical condition and the "Non-obese" mice treated with NFD as the healthy control. HFD mice are significantly larger in body weight compared with NFD mice (Supplementary Fig. 12A). The intraperitoneal glucose tolerance test (IPGTT) on the final day showed a trend towards insulin resistance (Supplementary Fig. 12B), but the blood glucose level was < 200 after 2 hours, which does not meet the diagnostic criteria for T2D [Winzell and Ahren (2004); Srinivasan and Ramarao (2007)]. I observed an obesity-associated increase in the methylation level in the spleen, adipose tissue and PBCs (Fig. 5D). I also observed that the methylation level gradually increased in accordance with the increase over the weeks of treatment with the HFD (Supplementary Fig. 13).

Chapter 3: Expression analysis of Elovl2 and Klf14

As I detected the rise in age-related methylation in *Elovl2* and *Klf14,* I examined the expression levels in *Elovl2* and *Klf14* in different ages. I quantitated the expression levels of *Elovl2* using quantitative reverse transcription PCR using the cDNA sampled from the lung, spleen and colon; however, *Elovl2* transcripts were undetectable in these organs from both "Young" and the "Aged" mice (the results of the colon are shown in Supplementary Fig. 14). These results are consistent with a previous study reporting that this gene is expressed in brain, liver, pancreas and testis, but not in the lung, colon or spleen [Berdasco and Esteller (2012)]. Hence, some organs such as brain, liver, pancreas and testis might be free from age-related DNA methylation in *Elovl2*.

Similarly, cDNA sampled from the spleen, adipose tissue and PBCs was used to examine the

expression levels of *Klf14*. *Klf14* is known to be expressed in various organs in addition to adipose tissue [Parker-Katiraee et al. (2007)]. I examined the expression levels of *Klf14* in the adipose tissue in "Young" and "Aged" male B6 mice. I observed a significant decrease in the gene expression of *Klf14* in the "Aged" mice (Fig. 6A). This age-related reduction of gene expression might have been due to the age-related increase in methylation levels in the promoter region of *Klf14*, as shown in Fig. 5A. I also examined the expression levels of *Klf14* in the adipose tissue in "T2D" and "Healthy" male mice. I observed a significant decrease in the gene expression of *Klf14* in the "T2D" mice (Fig. 6B). This result also revealed that the significant decrease in gene expression correlated with the increase in T2D-related methylation as well as age. I further examined the expression levels of *Klf14* in the adipose tissue in "Obese" and "Non-obese" male B6 mice. I observed a significant reduction of the gene expression of *Klf14* in the "Obese" mice (Fig. 6C). The same result was obtained for PBCs. Therefore, with regard to *Klf14*, gene expression declined with increasing methylation in all mice in this study.

Chapter 4: Expression analysis of downstream genes of Klf14 and cytokine analysis

KLF14 is a transcription factor that is known to be a master regulator of many downstream genes, including inflammatory genes [Grarup et al. (2010); Voight et al. (2010); Small et al. (2011); Civelek and Lusis. (2014)]. Therefore, I quantified the expression levels of 6 downstream genes (i.e., *Prmt2*, *Klf13*, *Gnb1*, *Temt*, *Slc7a* and *Ninj2*) and 6 inflammatory genes (i.e., *Adipoq*, *Tnf-a*, *Il-12*, *Il-6*, *Foxp3* and *F4/80*) in the adipose tissue in "Obese" and "Non-obese" mice. I observed significant changes in the expression levels of these genes between the "Obese" and "Non-obese" mice, except for *Gnb1* (Fig. 6D). The expression of all genes exhibited a significant decrease in "Obese" mice, with the exception of three inflammatory genes: *Tnf-α,* Il-12 and Il-6. The largest changes are observed in two inflammatory genes: a 7-fold increase in *Il-12* and a 3-fold increase in *Tnf-α*. Interestingly, *Adipoq* and *Foxp3* are reported as anti-inflammation gene [Dalmas et al. (2015)]. This result suggested that *Klf14* simultaneously reduced anti-inflammatory molecules and increased inflammatory molecules and that *Klf14* was related not only to the metabolism in adipose tissue but also to inflammation, as suggested in

previous studies [Fokeng et al (2016); Franks and McCarthy (2016)].

Due to the observation of increased expression in two inflammatory cytokine genes, *Il-12* and *Tnf-α* downstream of *Klf14* in the "Obese" mice, I quantified the amount of IL-12 and TNF-α as well as three additional cytokines, IFN-γ, IL-6 and IL-1α, by FACs analyses in the serum and stromal vascular fraction (SVF) of the adipose tissue. I observed no significant difference in cytokine expression in the serum between the "Obese" and the "Non-obese" mice, although two of them showed marginally significant increases: IL-6 (P = 0.054) and TNF-α (P = 0.055) (Fig. 7A). By contrast, I observed a significant obesity-related increase in all five cytokines tested in SVF (Fig. 7B). Although all five cytokines showed a significant obesity-related increase, the most responsive cytokines were TNF-α showing a 4-fold increase and IL-12 showing a 12-fold increase (Fig. 7B). IL-12 also showed the most significant decrease in gene expression in this study. IL-12 has recently been reported to be associated with differentiation into M1 macrophages [Dalmas et al. (2015)], My result suggests that expression levels of *Klf14* affects the differentiation into M1 macrophages in SVF. Although I failed to detect changes in inflammatory cytokines in serum, the inflammatory cytokines were significantly increased in adipose tissue, especially SVF. This result suggested that prediction of T2D at the subclinical stage might be difficult by inflammatory tests using peripheral blood materials.

Chapter 5: Methylation changes in mice returning to NFD from HFD

In addition to susceptible genes as genetic factors, physiological states such as chronological age, obesity and lack of exercise are contributing factors to the incidence of T2D. Dietary control and exercise are widely known to be effective to reduce the risk for T2D. To examine the significance of dietary change in methylation levels in *Klf14*, I prepared three different dietary conditions (Supplementary Fig. 2E). The first group consisted of male B6 mice raised only with a normal food diet (NFD) for 16 weeks ("N-only"). The second group contained male B6 mice raised with an NFD for 4 weeks and then a high fat diet (HFD) for 12 weeks ("N-H"). The third group comprised male B6 mice raised with an NFD for 4 weeks, then a HFD for 4 weeks and then again a NFD for 8 weeks ("N-H-N").

While the “N-H” mice showed the highest rate of weight gain, the “N-H-N” mice stopped gaining weight immediately after the switch back to NFD from HFD (Supplementary Fig. 15).

In adipose tissue, I observed a significant reduction of the methylation level at P3 of *Klf14* in “N-H-N” mice at 8 weeks after the dietary switch back to NFD from HFD, while the “N-H” mice showed a continuous increase in the methylation level (Fig. 8A). Body weight decreased immediately, and despite losing significance in “N-H-N” mice at 4 weeks after the dietary switch back to NFD from HFD, no significant decrease in methylation levels in “N-H-N” mice was detected at 4 weeks. Based on this result, weight loss was not necessarily accompanied by a decrease in the methylation of *Klf14* in adipose tissue, although it is considered important to maintain for a certain period.

In PBCs, I observed a weak but similar trend to that observed in adipose tissue. The reduction of the methylation level in “N-H-N” was significant only at 8 weeks after the dietary switch back to NFD from HFD (Fig. 8B). Consequently, the methylation level of *Klf14* in PBCs was correlated with the methylation of *Klf14* in adipose tissue.

Discussion

The EWAS presented herein using PBCs from Japanese cohorts identified novel age-associated CpG sites at 7 loci, 3q29, *C1R CC2D2A*, *OTUD7A*, *RASSF5*, *SERINC5*, *TRIM2*, and, as well as ten known loci, 1p13.2, *ELOVL2*, *FHL2*, *KLF14*, *KLHL35*, *MIR29B2*, *NHLRC1*, *PCDHB1*, *SFMBT1* and *TRIM59* [Rakyan et al. (2010); Bell et al. (2012); Garagnani et al. (2012); Hannum et al. (2013) Markunas et al. (2016]. Among the newly identified genes, some have been reported to be associated with human diseases. *CC2D2A* has been reported to play a critical role in the formation of cilia and to be associated with Meckel syndrome (MKS; MIM 249000), Joubert syndrome and related disorders (JSRD; MIM 213300), and autosomal-recessive mental retardation with retinitis pigmentosa (RP; MIM 268000) [Tallila et al. (2008); Gorden et al. 2008; Noor et al. (2008)]. MKS and JSRD belong to ciliopathies sharing common phenotypes (retinal dystrophy, polydactyly, cystic renal disease, and hepatic fibrosis) and molecular mechanisms [Gorden et al. (2008)]. *TRIM2* encodes UbcH5a-dependent ubiquitin ligase and is highly expressed in the nervous system. TRIM2 protein is known to bind to neurofilament light subunit (NF-L) and regulate its ubiquitination. *TRIM2*-deficient mice present increased levels of NF-L in axons and develop juvenile-onset ataxia [Balastik et al. (2008)]. *SERINC5* is abundantly expressed in myelin throughout the brain and facilitates the synthesis of both phosphatidylserine and sphingolipids [Inuzuka et al. (2005)]. A phosphatidylserine formulation has been shown to improve learning and memory tasks in patients with age-associated memory impairments [Crook et al. (1991)]. *C1R* is known to be associated with the development of systemic lupus erythematosus (SLE) [Zipfel and Skerta. (2009)].

The most significantly associated site was found in *ELOVL2,* which is responsible for the elongation of PUFA, including docosapentaenoic acid (DPA), eicosapentaenoic acid (EPA) and docosahexaenoic acid (DHA) [Leonard et al (2002); Ohno et al (2010)]. A genome-wide association study (GWAS) also demonstrated that *ELOVL2* is the susceptibility locus for plasma phospholipid levels of EPA, DPA, and DHA [Lemaitre et al. (2011)]. The n-3 long-chain PUFA, which is abundant in fish, has pleiotropic effects on biological functions, such as inhibition of platelet aggregation,

vasodilation, anti-inflammation, reduction of plasma triglyceride level, and anti-hypertensive effects. An epidemiological study has also reported that n-3 long-chain PUFA shows beneficial effects for cardiovascular disease, depression, Alzheimer's disease, and dementia [Riediger et al. (2009)]. *FHL2* is a member of the LIM-only protein family. Protein members within the group share highly conserved amino acid sequences, suggesting that the family members originated from a single ancestral gene copy [Fimia et al. (2000)]. These proteins are defined by the presence of the four and a half cysteine-rich LIM homeodomains, with the half-domain located in the N-terminus [Kurakula et al. (2015)]. *FHL2* has been reported to be associated with osteoporosis [Kurakula et al. (2015)]. *TRIM59* has been reported to be associated with tumorigenesis [Khatamianfar et al. (2012); Zhou et al. (2014)]. The overexpression of *Trim59* has been shown to repress signaling via NF-κB, Ifn-β, and the interferon-sensitive response element (ISRE) in mice [Kondo et al. (2012)]. *KLF14* is a member of the Krüppel-like factor family of transcription factors with zinc-finger domains capable of binding GC-rich sequences [Parker-Katiraee et al. (2007); Small et al. (2011)]. *KLF14* regulates the transcription levels of various genes, including the type II receptor for transforming growth factor-beta (TGFβRII) [Truty et al. (2009)]. *KLF14* is also known to be a master regulator of inflammatory genes in adipose tissue and to be associated with BMI and adult-onset diseases such as T2D, coronary artery disease and hypercholesterolemia [Parker-Katiraee et al. (2007); Grarup et al. (2010); Voight et al. (2010); Small et al. (2011)]. Age-associated methylation in the promoter region of *KLF14* has been previously reported in multiple human populations with different ethnic backgrounds [Garagnani et al. (2012); Hannum et al. (2013); Steegenga et al. (2014); Rönn et al. (2015); Kananen et al. (2016)]. The identification of these disease-susceptibility genes in EWAS with age suggests that age-associated changes in DNA methylation would not be merely biomarkers of aging but have an important role in the pathogenesis of a broad spectrum of diseases.

The age-related methylation changes in the CpG sites in the promoter regions in *ELOVL2* and *KLF14* in humans were shown to be replicated in mice. I showed that this change was organ-specific: the lung, spleen, colon and tail were responsive to age in terms of DNA methylation in the promoter

region of *Elovl2*. Although multiple EWASs as well as the present study have reported age-associated methylation changes in the promoter region of *ELOVL2* [Garagnani et al. (2012); Hannum et al. (2013); Rönn et al. (2015)], none have identified the responsible environmental factors affecting epigenetic changes among the suggested candidates, such as physical stresses and nutrients. It is almost impossible to assess epigenetic changes in various organs at different ages at the individual level in humans. Therefore, the results obtained using my mouse models provide unique information to understand the molecular process of age-associated DNA methylation in the *ELOVL2* promoter at an individual level.

The expression level of *Elovl2* was undetectable in any of the lung, spleen and colon in "Young" and "Aged" mice. A previous study has reported that this gene is expressed in liver, pancreas and testis, but not in the lung, colon or spleen [Ohno et al. (2010)], which is consistent with my current results. One possibility is that the target gene expression level is regulated by the age-associated methylation of neighboring genes. In the human genome, a neighboring gene, *ELOVL2-AS1,* shares a promoter region with *ELOVL2*. However, because *Elovl2-as1* is not annotated in the current mouse genome data (mm9), I could not evaluate the expression of this gene. This gene will be examined in future experiments. Another possibility is that this age-associated methylation change is merely an accidental result of aging with no functional significance. However, since these organ-specific epigenetic changes are evolutionarily conserved at least between human and mouse, they are likely to retain functional significance. As the most significant methylation change in *Elovl2* was observed in the colon, it is possible that the unknown function of *Elovl2* is associated with the colon. The histological study analyzing each cell type in normal and abnormal colon tissue, such as cancer cells, might be helpful to clarify the function of age-related methylation in *ELOVL2*.

The age-associated methylation changes at CpG sites in *Fhl2* and Trim59 originally observed in my human EWAS were not replicated in my mouse experiments. These discrepancies can be attributed to the biological differences between mouse and human, such as the distinct functions of orthologs, physiology, genomic context of the region and process of aging, in addition to the experimental differences between the two species, including genetically uniform mice in controlled environments and

genetically heterogeneous humans in heterogeneous environments.

I showed that *KLF14* represented another gene in which the age-related methylation changes were shared by humans and mice. *KLF14* has also been reported to be significant age-responsive genes by previous EWASs in human samples [Garagnani et al. (2012); Hannum et al. (2013); Steegenga et al. (2014); Rönn et al. (2015); Bacos et al. (2016); Kananen et al. (2016)]. Additionally, *KLF14* has been reported to be associated with T2D in large GWASs [Manolio et al. (2008); Imamura and Maeda (2011); Morris et al. (2012); Flannick and Florez (2016)]. Utilizing the advantages of animal models, I could examine methylation changes in *Klf14* in multiple organs collected from environmentally controlled individuals of different ages. The spleen, colon, kidneys, adipose tissues and PBCs were the most responsive organs to DNA methylation of *Klf14*. A previous study has reported that *KLF14* is expressed in spleen, colon, kidneys and adipose tissues [Parker-Katiraee et al. (2007)], which is consistent with my results. Therefore, in the present study, I demonstrated that the methylation-associated reduction in gene expression of *Klf14* occurred in spleen, adipose tissue and PBCs. Furthermore, the decrease in expression of *Klf14* in spleen, adipose tissue and PBCs was correlated with the decrease in expression of the downstream gene set regulated by *Klf14*. These downstream genes also have been reported to be associated with BMI, HDL cholesterol, TG, waist–hip ratio: WHR, insulin sensitivity, inflammation and HOMA-IR in GWASs with large sample sizes [Fokeng et al. (2016); Franks and McCarthy (2016)]. In the current study, however, I could not detect significant differences in HDL cholesterol, TG or HOMA-IR, although I detected significant differences in weight, insulin sensitivity and inflammation.

As *KLF14* is known to be a master regulator of inflammatory genes, the significantly altered expression of inflammatory genes such as *Tnf-α* and *IL-12* could be reasonably attributed to the significant obesity-associated decrease in *Klf14* gene expression, suggesting a global change in the inflammatory status of adipose tissue in T2D as well as obese mice. My results are also consistent with previous studies reporting that age, T2D and HFD exacerbate inflammation [Wu et al. (2007)]. It is notable that the most responsive cytokine is Il-12 that is known to be involved in the differentiation of

naive T cells into Th1 cells [Hsieh et al. (1993); Dalmas et al. (2015)]. Interestingly, *Klf14* has also been reported to be associated with the differentiation of regulatory T cells and macrophages [Sarmento et al. (2015)]. Future studies are required to identify the responsible cell types and to clarify the mechanisms underlying the inflammatory change triggered by the methylation change in adipose tissue.

One of the major treatments for early T2D to recover insulin sensitivity is dietary therapy by reducing calorie intake. In this study, I showed that the weight and methylation level of *Klf14* were gradually increased by the 4-week HFD treatment and that gaining weight stopped after the dietary improvement, i.e., the switch from HFD to NFD (Supplementary Fig. 15). However, it took 8 weeks to recover the increased methylation level to normal levels after the 4-week HFD treatment, although an improvement was observed during the first 4 weeks (Fig. 8). Since the chronological ages of humans are significantly longer than mice although the precise conversion is difficult, my results indicate that humans require a long time to recover the weight gain after diet therapy and even longer time to recover the methylation level in *Klf14*. For precise estimation of the length of the period to recover the epigenetic status that is potentially useful for clinical purposes, it is necessary to examine mice in a greater variety of dietary combinations with different durations of HFD and NFD treatments.

Due to the explosive increase in T2D patients worldwide, highly specific and highly sensitive biomarkers are demanded to identify people in subclinical states of T2D. Considering the evolutionary conservation of the epigenetic changes in *KLF14*, I consider *KLF14* a hopeful candidate as an epigenetic biomarker to predict inflammatory changes in adipose tissue. Since the epigenetic changes in *KLF14* were shown to also be associated with inflammation, *KLF14* may serve as a biomarker for other metabolic diseases involving inflammation in addition to T2D. It is notable that the epigenetic changes in *KLF14* were detectable in PBCs, which is one of the easiest tissues to access. Therefore, *Klf14* could be a predictive epigenetic biomarker for age-related multifunctional diseases including T2D. Further studies are necessary to clarify the mechanism underlying the epigenetic changes during disease.

Conclusion

Using an EWAS, I identified 22 CpG sites located in 17 loci that showed significant age-associated changes in DNA methylation. I showed that the age-associated DNA methylation changes in *Elovl2* and *Klf14* were conserved in mice. The methylation levels of *Elovl2* and *Klf14* increased with age, especially in the lung, spleen and colon, similarly to in human PBCs. The methylation level of mouse *Klf14* was associated with T2D and obesity as well as aging, especially in adipose tissue, spleen and PBCs. It is notable that the increased methylation level of *Klf14* introduced by HFD could be reversed to the normal levels by switching back to NFD and that the methylation changes could be detected in subclinical states in PBCs, one of the easiest tissues to access. Therefore, I conclude that methylation changes in *KLF14* may serve as a predictive epigenetic biomarker for age-associated multifunctional diseases such as T2D in the clinic.

Acknowledgements

I would like to express my gratitude to Prof. Toyoshi Inoguchi, FUKUOKA Health Promotion Support Center, for providing extensive advice and encouragement for this thesis. I also would like to express my gratitude to Assoc. Prof. Hiroki Shibata, Division of Genomics, Medical Institute of Bioregulation, Kyushu University, for supervising this thesis. I am deeply grateful to Prof. Ken Yamamoto, Department of Medical Biochemistry, Kurume University School of Medicine, for providing important advice for this thesis. I would like to thank Dr. Hidetoshi Kitajima, Wellcome Centre for Human Genetics, University of Oxford, Oxford, UK, for statistical and bioinformatics analysis. I also thank Dr. Yasutaka Maeda, Clinical Research Center for Diabetes, Clinic Masae Minami, for warm encouragement and support. I also thank Dr. Noriyuki Sonoda, Department of Medicine and Bioregulatory Science, Kyushu University, for encouragement, and Ms. Miki Sonoda for her technical assistance. Finally, I want to thank my parents for warm encouragement and support.

Funding

This study was supported by KAKENHI Grant Number 15 K08290 from the Japan Society for the Promotion of Science (JSPS) (K.Y), Research Fellowships from JSPS for Young Scientists (C.I. #20160345) and Manpei Suzuki Diabetes Foundation Grant-in-Aid for young scientists working abroad (H.K.). This work was also supported in part by a grant for Creation of Innovation Centers for Advanced Interdisciplinary Research Areas Program from the Ministry of Education, Culture, Sports, Science and Technology of Japan (Funding program “Innovation Center for Medical Redox Navigation”) (Y.M, N.S, and T.I).

References

1. Asano H, Izaka H, Nagata K, Nakatochi M, Kobayashi M, Hirashiki A, Shintani S, Nishizawa T, Tanimura D, Naruse K, Matsubara T, Murohara T, Yokota M. Plasma resistin concentration determined by common variants in the resistin gene and associated with metabolic traits in an aged Japanese population. Diabetologia. 53: 234-46 (2010).

2. Bacos K, Gillberg L, Volkov P, Olsson AH, Hansen T, Pedersen O, Gjesing AP, Eiberg H, Tuomi T, Almgren P, Groop L, Eliasson L, Vaag A, Dayeh T, Ling C. Blood-based biomarkers of age-associated epigenetic changes in human islets associate with insulin secretion and diabetes. Nat Commun. 7: 11089 (2016).

3. Balastik M, Ferraguti F, Pires-da Silva A, Lee TH, Alvarez-Bolado G, Lu KP, Gruss P. Deficiency in ubiquitin ligase TRIM2 causes accumulation of neurofilament light chain and neurodegeneration. Proc Natl Acad Sci U S A. 105: 12016-12021 (2008).

4. Bell JT, Tsai PC, Yang TP, Pidsley R, Nisbet J, Glass D, Mangino M, Zhai G, Zhang F, Valdes A, Shin SY, Dempster EL, Murray RM, Grundberg E, Hedman AK, Nica A, Small KS, MuTHER Consortium, Dermitzakis ET, McCarthy MI, Mill J, Spector TD, Deloukas P. Epigenome-wide scans identify differentially methylated regions for age and age-related phenotypes in a healthy ageing population. PLoS Genet. 8: e1002629 (2012).

5. Berdasco M, Esteller M. Hot topics in epigenetic mechanisms of aging: Aging Cell. 11: 181-186 (2012).

6. Bernstein BE, Meissner A, Lander ES. The mammalian epigenome. Cell. 128: 669-81 (2007).

7. Chan EM, Young EJ, Ianzano L, Munteanu I, Zhao X, Christopoulos CC, Avanzini G, Elia M, Ackerley CA, Jovic NJ, Bohlega S, Andermann E, Rouleau GA, Delgado-Escueta AV, Minassian BA, Scherer SW. Mutations in NHLRC1 cause progressive myoclonus epilepsy. Nat Genet. 35: 125–127 (2003).

8. Civelek M, Lusis AJ. Systems genetics approaches to understand complex traits. Nat Rev Genet. 15: 34-48 (2014).

9. Crook TH, Tinklenberg J, Yesavage J, Petrie W, Nunzi MG, Massari DC. Effects of phosphatidylserine in age-associated memory impairment. Neurology. 41: 644-649 (1991).

10. Dalmas E, Toubal A, Alzaid F, Blazek K, Eames HL, Lebozec K, Pini M, Hainault I, Montastier E, Denis RG, Ancel P, Lacombe A, Ling Y, Allatif O, Cruciani-Guglielmacci C, André S, Viguerie N, Poitou C, Stich V, Torcivia A, Foufelle F, Luquet S, Aron-Wisnewsky J, Langin D, Clément K, Udalova IA, Venteclef N. Irf5 deficiency in macrophages promotes beneficial adipose tissue expansion and insulin sensitivity during obesity. Nat Med. 21: 610–618 (2015).

11. Fimia GM, De Cesare D, Sassone-Corsi P. A family of LIM-only transcriptional coactivators: tissue-specific expression and selective activation of CREB and CREM. Mol Cell. 20: 8613–8622 (2000).

12. Flannick J, Florez JC. Type 2 diabetes: genetic data sharing to advance complex disease research. Nat Rev Genet. 17: 535-549 (2016).

13. Fokeng MG, Atogho Tiedeu B, Sobngwi E, Mbanya JC, Mbacham WF. The Kruppel-Like Factor 14 (KLF14), master gene of multiple metabolic phenotypes: putative trans-regulator network. Transl Biomed. 7: 2. (2016).

14. Franks PW, McCarthy MI. Exposing the exposures responsible for type 2 diabetes and obesity. Science. 354: 69–73 (2016).

15. Garagnani P, Bacalini MG, Pirazzini C, Gori D, Giuliani C, Mari D, Di Blasio AM, Gentilini D, Vitale G, Collino S, Rezzi S, Castellani G, Capri M, Salvioli S, Franceschi C. Methylation of *ELOVL2* gene as a new epigenetic marker of age. Aging Cell. 11: 1132-1134 (2012).

16. Gorden NT, Arts HH, Parisi MA, Coene KL, Letteboer SJ, van Beersum SE, Mans DA, Hikida A, Eckert M, Knutzen D, Alswaid AF, Ozyurek H, Dibooglu S, Otto EA, Liu Y, Davis EE, Hutter CM, Bammler TK, Farin FM, Dorschner M, Topçu M, Zackai EH, Rosenthal P, Owens KN, Katsanis N, Vincent JB, Hildebrandt F, Rubel EW, Raible DW, Knoers NV, Chance PF, Roepman R, Moens CB, Glass IA, Doherty D. CC2D2A is mutated in Joubert syndrome and interacts with the ciliopathy-associated basal body protein CEP290. Am J Hum. Genet. 83: 559-571 (2008).

17. Grarup N, Sparsø T, Hansen T. Physiologic characterization of type 2 diabetes-related loci. Curr Diab Rep. 10: 485–497 (2010).

18. Günther T, Poli C, Müller JM, Catala-Lehnen P, Schinke T, Yin N, Vomstein S, Amling M, Schüle R. Fhl2 deficiency results in osteopenia due to decreased activity of osteoblasts. EMBO J. 24: 3049-3056 (2005)

19. Gut P, Verdin E. The nexus of chromatin regulation and intermediary metabolism. Nature. 502: 489-498. (2013)

20. Hannum G, Guinney J, Zhao L, Zhang L, Hughes G, Sadda S, Klotzle B, Bibikova M, Fan JB, Gao Y, Deconde R, Chen M, Rajapakse I, Friend S, Ideker T, Zhang K. Genome-wide methylation profiles reveal quantitative views of human aging rates. Mol Cell. 49: 359-367 (2013).

21. Hsieh CS, Macatonia SE, Tripp CS, Wolf SF, O'Garra A, Murphy KM. Development of TH1 CD4+ T cells through IL-12 produced by Listeria-induced macrophages. Science. 260: 547-549 (1993).

22. Imamura M, Maeda S. Genetics of type 2 diabetes: the GWAS era and future perspectives. Endocr J. 58: 723–739 (2011).

23. Inuzuka M., Hayakawa M, Ingi T. Serinc, an activity-regulated protein family, incorporates serine into membrane lipid synthesis. J Biol Chem. 280: 35776-35783 (2005).

24. Johannessen M, Møller S, Hansen T, Moens U, Van Ghelue M. The multifunctional roles of the four-and-a-half-LIM only protein FHL2. Cell Mol Life Sci. 63: 268–284 (2006).

25. Kananen L, Marttila S, Nevalainen T, Jylhävä J Mononen N, Kähönen M, Raitakari OT, Lehtimäki T, Hurme M. Aging-associated DNA methylation changes in middle-aged individuals: The Young Finns study. BMC Genomics. 17: 103 (2016).

26. Karolchik D, Hinrichs AS, Furey TS, Roskin KM, Sugnet CW, Haussler D, Kent WJ. The UCSC Table Browser data retrieval tool. Nucleic Acids Res. 32: D493-6 (2004).

27. Kent WJ, Sugnet CW, Furey TS, Roskin KM, Pringle TH, Zahler AM, Haussler D. The human

genome browser at UCSC. Genome Res. 12: 996-1006 (2002).

28. Khatamianfar V, Valiyeva F, Rennie PS, Lu WY, Yang BB, Bauman GS, Moussa M, Xuan JW. TRIM59, a novel multiple cancer biomarker for immunohistochemical detection of tumorigenesis. BMJ Open. 2: e001410 (2012).

29. Kondo T, Watanabe M, Hatakeyama S. TRIM59 interacts with ECSIT and negatively regulates NF-κB and IRF-3/7-mediated signal pathways. Biochem Biophys Res Commun. 422: 501-7 (2012).

30. Kurakula K, Vos M, van Eijk M, Smits HH, de Vries CJ. 31. LIM-only protein FHL2 regulates experimental pulmonary *Schistosoma mansoni* egg granuloma formation. Eur J Immunol. 45: 3098-106 (2015).

31. Lemaitre RN, Tanaka T, Tang W, Manichaikul A, Foy M, Kabagambe EK, Nettleton JA, King IB, Weng LC, Bhattacharya S, Bandinelli S, Bis JC, Rich SS, Jacobs DR Jr, Cherubini A, McKnight B, Liang S, Gu X, Rice K, Laurie CC, Lumley T, Browning BL, Psaty BM, Chen YD, Friedlander Y, Djousse L, Wu JH, Siscovick DS, Uitterlinden AG, Arnett DK, Ferrucci L, Fornage M, Tsai MY, Mozaffarian D, Steffen LM. Genetic loci associated with plasma phospholipid n-3 fatty acids: a meta-analysis of genome-wide association studies from the CHARGE Consortium. PLoS Genet. 7: e1002193 (2011).

32. Leonard AE, Kelder B, Bobik EG, Chuang LT, Lewis CJ, Kopchick JJ, Mukerji P, Huang YS. Identification and expression of mammalian long-chain PUFA elongation enzymes. Lipids. 37:

733-740 (2002).

33. Ling C, Groop L. Epigenetics: a molecular link between environmental factors and type 2 diabetes. Diabetes. 58: 2718-2725. (2009).

34. Manolio TA, Brooks LD, Collins FS. A HapMap harvest of insights into the genetics of common disease. J Clin Invest. 118: 1590-1605 (2008).

35. Manolio TA, Collins FS, Cox NJ, Goldstein DB, Hindorff LA, Hunter DJ, McCarthy MI, Ramos EM, Cardon LR, Chakravarti A, Cho JH, Guttmacher AE, Kong A, Kruglyak L, Mardis E, Rotimi CN, Slatkin M, Valle D, Whittemore AS, Boehnke M, Clark AG, Eichler EE, Gibson G, Haines JL, Mackay TF, McCarroll SA, Visscher PM. Finding the missing heritability of complex diseases. Nature. 461: 747–753 (2009).

36. Markunas CA, Wilcox AJ, Xu Z, Joubert BR, Harlid S, Panduri V, Håberg SE, Nystad W, London SJ, Sandler DP, Lie RT, Wade PA, Taylor JA. Maternal age at delivery is associated with an epigenetic signature in both newborns and adults. PLoS One. 11: e0156361 (2016).

37. Michels KB, Binder AM, Dedeurwaerder S, Epstein CB, Greally JM, Gut I, Houseman EA, Izzi B, Kelsey KT, Meissner A, Milosavljevic A, Siegmund KD, Bock C, Irizarry RA. Recommendations for the design and analysis of epigenome-wide association studies. Nat Methods. 10: 949-955 (2013).

38. Morgan E, Varro R, Sepulveda H, Ember JA, Apgar J, Wilson J, Lowe L, Chen R, Shivraj L, Agadir A, Campos R, Ernst D, Gaur A. Cytometric bead array: a multiplexed assay platform with

applications in various areas of biology. Clin Immunol. 110: 252-266 (2004).

39. Morris AP, Voight BF, Teslovich TM, Ferreira T, Segrè AV, Steinthorsdottir V, Strawbridge RJ, Khan H, Grallert H, Mahajan A, Prokopenko I, Kang HM, Dina C, Esko T, Fraser RM, Kanoni S, Kumar A, Lagou V, Langenberg C, Luan J, Lindgren CM, Müller-Nurasyid M, Pechlivanis S, Rayner NW, Scott LJ, Wiltshire S, Yengo L, Kinnunen L, Rossin EJ, Raychaudhuri S, Johnson AD, Dimas AS, Loos RJ, Vedantam S, Chen H, Florez JC, Fox C, Liu CT, Rybin D, Couper DJ, Kao WH, Li M, Cornelis MC, Kraft P, Sun Q, van Dam RM, Stringham HM, Chines PS, Fischer K, Fontanillas P, Holmen OL, Hunt SE, Jackson AU, Kong A, Lawrence R, Meyer J, Perry JR, Platou CG, Potter S, Rehnberg E, Robertson N, Sivapalaratnam S, Stančáková A, Stirrups K, Thorleifsson G, Tikkanen E, Wood AR, Almgren P, Atalay M, Benediktsson R, Bonnycastle LL, Burtt N, Carey J, Charpentier G, Crenshaw AT, Doney AS, Dorkhan M, Edkins S, Emilsson V, Eury E, Forsen T, Gertow K, Gigante B, Grant GB, Groves CJ, Guiducci C, Herder C, Hreidarsson AB, Hui J, James A, Jonsson A, Rathmann W, Klopp N, Kravic J, Krjutškov K, Langford C, Leander K, Lindholm E, Lobbens S, Männistö S, Mirza G, Mühleisen TW, Musk B, Parkin M, Rallidis L, Saramies J, Sennblad B, Shah S, Sigurðsson G, Silveira A, Steinbach G, Thorand B, Trakalo J, Veglia F, Wennauer R, Winckler W, Zabaneh D, Campbell H, van Duijn C, Uitterlinden AG, Hofman A, Sijbrands E, Abecasis GR, Owen KR, Zeggini E, Trip MD, Forouhi NG, Syvänen AC, Eriksson JG, Peltonen L, Nöthen MM, Balkau B, Palmer CN, Lyssenko V, Tuomi T, Isomaa B, Hunter DJ, Qi L. Wellcome Trust Case Control Consortium. Meta-Analyses of Glucose and Insulin-related traits

Consortium (MAGIC) Investigators, Genetic Investigation of ANthropometric Traits (GIANT) Consortium; Asian Genetic Epidemiology Network–Type 2 Diabetes (AGEN-T2D) Consortium, South Asian Type 2 Diabetes (SAT2D) Consortium, Shuldiner AR, Roden M, Barroso I, Wilsgaard T, Beilby J, Hovingh K, Price JF, Wilson JF, Rauramaa R, Lakka TA, Lind L, Dedoussis G, Njølstad I, Pedersen NL, Khaw KT, Wareham NJ, Keinanen-Kiukaanniemi SM, Saaristo TE, Korpi-Hyövälti E, Saltevo J, Laakso M, Kuusisto J, Metspalu A, Collins FS, Mohlke KL, Bergman RN, Tuomilehto J, Boehm BO, Gieger C, Hveem K, Cauchi S, Froguel P, Baldassarre D, Tremoli E, Humphries SE, Saleheen D, Danesh J, Ingelsson E, Ripatti S, Salomaa V, Erbel R, Jöckel KH, Moebus S, Peters A, Illig T, de Faire U, Hamsten A, Morris AD, Donnelly PJ, Frayling TM, Hattersley AT, Boerwinkle E, Melander O, Kathiresan S, Nilsson PM, Deloukas P, Thorsteinsdottir U, Groop LC, Stefansson K, Hu F, Pankow JS, Dupuis J, Meigs JB, Altshuler D, Boehnke M, McCarthy MI, DIAbetes Genetics Replication And Meta-analysis (DIAGRAM) Consortium. Large-scale association analysis provides insights into the genetic architecture and pathophysiology of type 2 diabetes. Nat Genet. 44: 981-990 (2012).

40. Nanri A, Mizoue T, Yoshida D, Takahashi R, Takayanagi R. Dietary patterns and A1C in Japanese men and women. Diabetes Care. 31: 1568-73 (2008).

41. Noor A, Windpassinger C, Patel M, Stachowiak B, Mikhailov A, Azam M, Irfan M, Paterson AD, Lutufullah M, Doherty D, Vincent JB, Ayub M. CC2D2A, encoding a coiled-coil and C2 domain protein, causes autosomal-recessive mental retardation with retinitis pigmentosa. Am J Hum Genet.

82: 1011-1018 (2008).

42. Ohnaka K, Kono S, Inoguchi T, Yin G, Morita M, Adachi M, Kawate H, Takayanagi R. Inverse associations of serum bilirubin with high sensitivity C-reactive protein, glycated hemoglobin, and prevalence of type 2 diabetes in middle-aged and elderly Japanese men and women. Diabetes Res Clin Pract. 88:103-10 (2010).

43. Ohno Y, Suto S, Yamanaka M, Mizutani Y, Mitsutake S, Igarashi Y, Sassa T, Kihara A. ELOVL1 production of C24 acyl-CoAs is linked to C24 sphingolipid synthesis. Proc Natl Acad Sci U S A. 107: 18439-18444 (2010).

44. Parker-Katiraee L, Carson AR, Yamada T, Arnaud P, Feil R, Abu-Amero SN, Moore GE, Kaneda M, Perry GH, Stone AC, Lee C, Meguro-Horike M, Sasaki H, Kobayashi K, Nakabayashi K, Scherer SW. Identification of the imprinted KLF14 transcription factor undergoing human-specific accelerated evolution. PLoS Genet. 3: e65 (2007).

45. Rakyan VK, Down TA, Maslau S, Andrew T, Yang TP, Beyan H, Whittaker P, McCann OT, Finer S, Valdes AM, Leslie RD, Deloukas P, Spector TD. Human aging-associated DNA hypermethylation occurs preferentially at bivalent chromatin domains. Genome Res. 20: 434-439 (2010).

46. Rakyan VK, Down TA, Balding DJ, Beck S. Epigenome-wide association studies for common human diseases. Nat Rev Genet. 12: 529-541 (2011).

47. Richardson B. Impact of aging on DNA methylation. Ageing Res Rev. 2: 245-261 (2003).

48. Riediger ND, Othman RA, Suh M, Moghadasian MH. A systemic review of the roles of n-3 fatty

acids in health and disease. J Am Diet Assoc. 109: 668-679 (2009).

49. Rönn T, Volkov P, Gillberg L, Kokosar M, Perfilyev A, Jacobsen AL, Jørgensen SW, Brøns C, Jansson PA, Eriksson KF, Pedersen O, Hansen T, Groop L9, Stener-Victorin E, Vaag A, Nilsson E, Ling C. Impact of age, BMI and HbA1c levels on the genome-wide DNA methylation and mRNA expression patterns in human adipose tissue and identification of epigenetic biomarkers in blood. Hum Mol Genet. 24: 3792-3813 (2015).

50. Sarmento OF, Svingen PA, Xiong Y, Xavier RJ, McGovern D, Smyrk TC, Papadakis KA, Urrutia RA, Faubion WA. A novel role for Kruppel-like factor 14 (KLF14) in T-regulatory cell differentiation. Cell Mol Gastroenterol Hepatol. 1: 188-202, e4 (2015).

51. Shinawi M, Schaaf CP, Bhatt SS, Xia Z, Patel A, Cheung SW, Lanpher B, Nagl S, Herding HS, Nevinny-Stickel C, Immken LL, Patel GS, German JR, Beaudet AL, Stankiewicz P. A small recurrent deletion within 15q13.3 is associated with a range of neurodevelopmental phenotypes. Nat Genet. 41: 1269–1271 (2009).

52. Singh A, Ganesh S. Lafora progressive myoclonus epilepsy: A meta-analysis of reported mutations in the first decade following the discovery of the EPM2A and NHLRC1 genes. Hum. Mutat. 30: 715–723. (2009).

53. Shinawi M, Schaaf CP, Bhatt SS, Xia Z, Patel A, Cheung SW, Lanpher B, Nagl S, Herding HS, Nevinny-Stickel C, Immken LL, Patel GS, German JR, Beaudet AL, Stankiewicz P. A small recurrent deletion within 15q13.3 is associated with a range of neurodevelopmental phenotypes.

Nat Genet. 41: 1269–1271 (2009).

54. Small KS, Hedman AK, Grundberg E, Nica AC, Thorleifsson G, Kong A, Thorsteindottir U, Shin SY, Richards HB; GIANT Consortium; MAGIC Investigators; DIAGRAM Consortium, Soranzo N, Ahmadi KR, Lindgren CM, Stefansson K, Dermitzakis ET, Deloukas P, Spector TD, McCarthy MI, MuTHER Consortium. Identification of an imprinted master trans regulator at the KLF14 locus related to multiple metabolic phenotypes. Nat Genet. 43: 561-564 (2011).

55. Srinivasan K, Ramarao P. Animal models in type 2 diabetes research: an overview Indian J Med Res. 125: 451-72 (2007).

56. Steegenga WT, Boekschoten MV, Lute C, Hooiveld GJ, de Groot PJ, Morris TJ, Teschendorff AE, Butcher LM, Beck S, Müller M. Genome-wide age-related changes in DNA methylation and gene expression in human PBMCs. Age 36: 1523–1540 (2014).

57. Tallila J, Jakkula E, Peltonen L, Salonen R, Kestila, M. Identification of CC2D2A as a Meckel syndrome gene adds an important piece to the ciliopathy puzzle. Am J Hum Genet. 82: 1361-1367 (2008).

58. Teslovich TM, Musunuru K, Smith AV, Edmondson AC, Stylianou IM, Koseki M, Pirruccello JP, Ripatti S, Chasman DI, Willer CJ, Johansen CT, Fouchier SW, Isaacs A, Peloso GM, Barbalic M, Ricketts SL, Bis JC, Aulchenko YS, Thorleifsson G, Feitosa MF, Chambers J, Orho-Melander M, Melander O, Johnson T, Li X, Guo X, Li M, Shin Cho Y, Jin Go M, Jin Kim Y, Lee JY, Park T, Kim K, Sim X, Twee-Hee Ong R, Croteau-Chonka DC, Lange LA, Smith JD, Song K, Hua Zhao J,

Yuan X, Luan J, Lamina C, Ziegler A, Zhang W, Zee RY, Wright AF, Witteman JC, Wilson JF, Willemsen G, Wichmann HE, Whitfield JB, Waterworth DM, Wareham NJ, Waeber G, Vollenweider P, Voight BF, Vitart V, Uitterlinden AG, Uda M, Tuomilehto J, Thompson JR, Tanaka T, Surakka I, Stringham HM, Spector TD, Soranzo N, Smit JH, Sinisalo J, Silander K, Sijbrands EJ, Scuteri A, Scott J, Schlessinger D, Sanna S, Salomaa V, Saharinen J, Sabatti C, Ruokonen A, Rudan I, Rose LM, Roberts R, Rieder M, Psaty BM, Pramstaller PP, Pichler I, Perola M, Penninx BW, Pedersen NL, Pattaro C, Parker AN, Pare G, Oostra BA, O'Donnell CJ, Nieminen MS, Nickerson DA, Montgomery GW, Meitinger T, McPherson R, McCarthy MI, McArdle W, Masson D, Martin NG, Marroni F, Mangino M, Magnusson PK, Lucas G, Luben R, Loos RJ, Lokki ML, Lettre G, Langenberg C, Launer LJ, Lakatta EG, Laaksonen R, Kyvik KO, Kronenberg F, König IR, Khaw KT, Kaprio J, Kaplan LM, Johansson A, Jarvelin MR, Janssens AC, Ingelsson E, Igl W, Kees Hovingh G, Hottenga JJ, Hofman A, Hicks AA, Hengstenberg C, Heid IM, Hayward C, Havulinna AS, Hastie ND, Harris TB, Haritunians T, Hall AS, Gyllensten U, Guiducci C, Groop LC, Gonzalez E, Gieger C, Freimer NB, Ferrucci L, Erdmann J, Elliott P, Ejebe KG, Döring A, Dominiczak AF, Demissie S, Deloukas P, de Geus EJ, de Faire U, Crawford G, Collins FS, Chen YD, Caulfield MJ, Campbell H, Burtt NP, Bonnycastle LL, Boomsma DI, Boekholdt SM, Bergman RN, Barroso I, Bandinelli S, Ballantyne CM, Assimes TL, Quertermous T, Altshuler D, Seielstad M, Wong TY, Tai ES, Feranil AB, Kuzawa CW, Adair LS, Taylor HA Jr, Borecki IB, Gabriel SB, Wilson JG, Holm H, Thorsteinsdottir U, Gudnason V, Krauss RM, Mohlke KL, Ordovas JM,

Munroe PB, Kooner JS, Tall AR, Hegele RA, Kastelein JJ, Schadt EE, Rotter JI, Boerwinkle E, Strachan DP, Mooser V, Stefansson K, Reilly MP, Samani NJ, Schunkert H, Cupples LA, Sandhu MS, Ridker PM, Rader DJ, van Duijn CM, Peltonen L, Abecasis GR, Boehnke M, Kathiresan S. Biological, clinical and population relevance of 95 loci for blood lipids. Nature. 466: 707-713 (2010).

59. Trerotola M, Relli V, Simeone P, Alberti S. Epigenetic inheritance and the missing heritability. Hum Genomics. 9: 17 (2015).

60. Truty MJ, Lomberk G, Fernandez-Zapico ME, Urrutia R. Silencing of the transforming growth factor-β (TGFβ) receptor II by Kruppel-like factor 14 underscores the importance of a negative feedback mechanism in TGFβ signaling. J Biol Chem. 284: 6291–6300 (2009).

61. Voight BF, Scott LJ, Steinthorsdottir V, Morris AP, Dina C, Welch RP, Zeggini E, Huth C, Aulchenko YS, Thorleifsson G, McCulloch LJ, Ferreira T, Grallert H, Amin N, Wu G, Willer CJ, Raychaudhuri S, McCarroll SA, Langenberg C, Hofmann OM, Dupuis J, Qi L, Segrè AV, van Hoek M, Navarro P, Ardlie K, Balkau B, Benediktsson R, Bennett AJ, Blagieva R, Boerwinkle E, Bonnycastle LL, Bengtsson Boström K, Bravenboer B, Bumpstead S, Burtt NP, Charpentier G, Chines PS, Cornelis M, Couper DJ, Crawford G, Doney AS, Elliott KS, Elliott AL, Erdos MR, Fox CS, Franklin CS, Ganser M, Gieger C, Grarup N, Green T, Griffin S, Groves CJ, Guiducci C, Hadjadj S, Hassanali N, Herder C, Isomaa B, Jackson AU, Johnson PR, Jørgensen T, Kao WH, Klopp N, Kong A, Kraft P, Kuusisto J, Lauritzen T, Li M, Lieverse A, Lindgren CM, Lyssenko V,

Marre M, Meitinger T, Midthjell K, Morken MA, Narisu N, Nilsson P, Owen KR, Payne F, Perry JR, Petersen AK, Platou C, Proença C, Prokopenko I, Rathmann W, Rayner NW, Robertson NR, Rocheleau G, Roden M, Sampson MJ, Saxena R, Shields BM, Shrader P, Sigurdsson G, Sparsø T, Strassburger K, Stringham HM, Sun Q, Swift AJ, Thorand B, Tichet J, Tuomi T, van Dam RM, van Haeften TW, van Herpt T, van Vliet-Ostaptchouk JV, Walters GB, Weedon MN, Wijmenga C, Witteman J, Bergman RN, Cauchi S, Collins FS, Gloyn AL, Gyllensten U, Hansen T, Hide WA, Hitman GA, Hofman A, Hunter DJ, Hveem K, Laakso M, Mohlke KL, Morris AD, Palmer CN, Pramstaller PP, Rudan I, Sijbrands E, Stein LD, Tuomilehto J, Uitterlinden A, Walker M, Wareham NJ, Watanabe RM, Abecasis GR, Boehm BO, Campbell H, Daly MJ, Hattersley AT, Hu FB, Meigs JB, Pankow JS, Pedersen O, Wichmann HE, Barroso I, Florez JC, Frayling TM, Groop L, Sladek R, Thorsteinsdottir U, Wilson JF, Illig T, Froguel P, van Duijn CM, Stefansson K, Altshuler D, Boehnke M, McCarthy MI. MAGIC investigators; GIANT Consortium. Twelve type 2 diabetes susceptibility loci identified through large scale association analysis. Nat Genet. 42: 579–589 (2010).

62. Winzell MS, Ahren B. The high-fat diet-fed mouse: a model for studying mechanisms and treatment of impaired glucose tolerance and type 2 diabetes. Diabetes 53 Suppl 3: S215-219 (2004).

63. Wu D, Ren Z, Pae M, Guo W, Cui X, Merrill AH, Meydani SN. Aging up-regulates expression of inflammatory mediators in mouse adipose tissue. J Immunol. 179: 4829–39 (2007).

64. Zhou Z, Ji Z, Wang Y, Li J, Cao H, Zhu HH, Gao WQ. TRIM59 is up-regulated in gastric tumors, promoting ubiquitination and degradation of p53. Gastroenterology 147: 1043-54 (2014).

65. Zipfel PF, Skerka C. Complement regulators and inhibitory proteins. Nat Rev Immunol. 9: 729-40 (2009).

Figure Legends

Figure 1. Scatter plots of the methylation changes at 17 representative loci showing significant associations with chronological age in the cumulative sample set. IDs of CpG sites are indicated with gene symbols in parantheses. Linear regression lines are also indicated with correlation coefficients (R).

Figure 2. The age-associated methylation site cg24724428 in the promoter region of *ELOVL2*. The age-associated CpG sites in human and the corresponding mouse site are marked by bold letters. The asterisks show conserved nucleotides in mouse. The predicted sequence after bisulfite treatment is shown at the bottom. The position of primers for PCR and pyrosequencing are highlighted by shadows and underlining, respectively. There are 9 CpG sites, P1-P9, located in the mouse target region of *Elovl2*. P4 is the site corresponding to cg24724428 in human.

Figure 3. The age-associated methylation site cg14361627 in the promoter region of *KLF14* depicted as in Figure 2 except a pyrosequencing primer. There are 9 CpG sites, P1-P9, located in the mouse target region of *Kfl14*. P1 is the site corresponding to cg14361627 in human.

Figure 4. Organ-specific methylation changes in the CpG sites in *Elovl2* (A) DNA methylation levels at P3 in various organs from the “Young” and “Aged" mice. The pooled results from male and female mice are shown. (B) The methylation levels at P1-P4 in the colon and spleen from the “Young” and “Aged” mice. (C) Results of bisulfite cloning-sequencing of the 9 CpG sites, including the additional 5 sites. Open and filled ellipses indicate non-methylated and methylated states, respectively. Each row corresponds to each clone. A total of 86 clones were analyzed for the DNA from colon of the “Young” and “Aged” mice. Five mice were used in each condition (*$P < 0.05$, **$P < 0.01$, ***$P < 0.005$. Error bars represent means ± SD).

Figure 5. DNA methylation levels in *Klf14* in different organs. DNA was analyzed for 36 clones. (A) Comparison of the methylation levels at multiple CpG sites (P1-P9) in *Klf14* in PBC between diet-matched “Young” and “Aged” male B6 mice. (B) Comparison of the methylation levels at P3 in *Klf14* in various organs between diet-matched “Young” and “Aged” male B6 mice. (C) Comparison of the methylation levels at P3 in *Klf14* in 3 organs, spleen, adipose tissue and PBC, between age-matched “T2D” and “Healthy” male mice. (D) Comparison of the methylation levels at P3 in *Klf14* in 3 organs, spleen, adipose tissue and PBC, between age-matched “Obese” and “Non-obese” male B6 mice. Five mice were used in each condition (*$P < 0.05$, **$P < 0.01$, ***$P < 0.005$. Error bars represent means ± SD).

Figure 6. The expression level of *Klf14* and related genes in adipose tissue quantitated by quantitative reverse transcription PCR. (A) Comparison of the mRNA expression of *Klf14* between diet-matched "Young" and "Aged" male B6 mice. (B) Comparison of the mRNA expression of *Klf14* between age- and diet-matched "Healthy" and "T2D" male mice. (C) The mRNA expression of *Klf14* in "Obese" mice normalized to the expression level in age-matched "Non-obese" mice. (D) The mRNA expression of downstream genes regulated by *Klf14* in age- and diet-matched "Healthy" and "T2D" male mice. Five mice were used in each condition (*$P < 0.05$, **$P < 0.01$, ***$P < 0.005$. Error bars represent means ± SD).

Figure 7. Five cytokines, IFN-γ, IL-6, TNF-α, IL-12 and IL-1β, were quantified by flow cytometry. (A) Comparison of the cytokine levels in serum between "Obese" and the "Non-obese" mice. (B) Comparison of the amounts of cytokines in SVF from adipose tissue between "Obese" and the "Non-obese" mice. Five mice were used in each condition (*$P < 0.05$, **$P < 0.01$, ***$P < 0.005$. Error bars represent means ± SD).

Figure 8. DNA methylation levels in *Klf14* in three different dietary conditions . DNA was analyzed for 36 clones. (A) DNA methylation levels at P3 in *Klf14* in adipose tissue. (B) DNA methylation levels at P3 in *Klf14* in PBC. Five mice were used in each condition.(*$P < 0.05$, **$P < 0.01$, ***$P < 0.005$. Error bars represent means ± SD).

Table 1. CpG sites with the methylation levels significantly associated with age.

Rank	Site	Chr. band	Position	Genes (location)	Fukuoka Cohort Study		KING Study		Combined	
					Effect size	*P* value	Effect size	*P* value	Effect size	*P* value
12	cg16008966	1p13.2	114,761,794	-	-0.0025	6.9×10^{-13}	-0.0024	6.8×10^{-8}	-0.0025	1.7×10^{-20}
20	cg08128734	1q32.1	206,685,423	*RASSF5* (intron)	-0.0027	4.1×10^{-8}	-0.0047	5.6×10^{-12}	-0.0033	1.5×10^{-16}
19	cg10501210	1q32.2	207,997,020	*MIR29B2* (0.97 kb upstream)	-0.0053	8.7×10^{-10}	-0.0068	3.6×10^{-8}	-0.0058	1.3×10^{-16}
2	cg06639320	2q12.2	106,015,739	*FHL2* (0.08 kb upstream)	0.0036	2.5×10^{-26}	0.0043	2.3×10^{-15}	0.0039	2.8×10^{-40}
3	cg22454769	2q12.2	106,015,767	*FHL2* (0.08 kb upstream)	0.0054	9.4×10^{-30}	0.0048	7.3×10^{-16}	0.0049	2.0×10^{-37}
4	cg24079702	2q12.2	106,015,771	*FHL2* (0.08 kb upstream)	0.0048	2.6×10^{-26}	0.0038	1.7×10^{-11}	0.0042	5.3×10^{-31}
14	cg03607117	3p21.1	53,080,440	*SFMBT1* (0.35 kb upstream)	0.0015	8.4×10^{-13}	0.0018	8.2×10^{-8}	0.0016	6.6×10^{-19}
5	cg07553761	3q25.33	160,167,977	*TRIM59* (0.35 kb upstream)	0.0040	1.0×10^{-21}	0.0046	9.4×10^{-19}	0.0038	3.6×10^{-28}
21	cg16932827	3q29	193,988,639	-	-0.0024	9.6×10^{-8}	-0.0034	6.8×10^{-8}	-0.0028	1.6×10^{-14}
22	cg20816447	4p15.32	15,480,781	*CC2D2A* (intron)	-0.0027	1.4×10^{-8}	-0.0035	9.0×10^{-8}	-0.0029	5.1×10^{-14}
16	cg10149533	4q31.3	154,064,784	*TRIM2* (9.5 kb downstream)	-0.0023	8.7×10^{-10}	-0.0037	4.9×10^{-11}	-0.0028	2.5×10^{-18}
17	cg06677021	5q14.1	79,490,511	*SERINC5* (intron)	0.0028	2.0×10^{-10}	0.0031	5.5×10^{-8}	0.0031	3.0×10^{-18}
8	cg23500537	5q31.3	140,419,819	*PCDHB1* (11 kb downstream)	0.0025	9.0×10^{-15}	0.0031	3.6×10^{-9}	0.0028	3.6×10^{-23}
1	cg16867657	6p24.2	11,044,877	*ELOVL2* (0.25 kb upstream)	0.0050	2.0×10^{-35}	0.0047	2.5×10^{-18}	0.0046	1.7×10^{-45}
11	cg24724428	6p24.2	11,044,888	*ELOVL2* (0.26 kb upstream)	0.0043	2.6×10^{-14}	0.0040	4.3×10^{-9}	0.0041	5.4×10^{-22}
9	cg21572722	6p24.2	11,044,894	*ELOVL2* (0.27 kb upstream)	0.0021	8.6×10^{-15}	0.0022	1.2×10^{-10}	0.0020	6.9×10^{-23}
10	cg22736354	6p22.3	18,122,719	*NHLRC1* (exon)	0.0023	1.7×10^{-17}	0.0022	8.2×10^{-8}	0.0022	2.3×10^{-22}
15	cg14361627	7q32.3	130,419,116	*KLF14* (0.23 kb upstream)	0.0027	6.8×10^{-13}	0.0027	9.1×10^{-9}	0.0026	1.6×10^{-19}
7	cg08097417	7q32.3	130,419,133	*KLF14* (0.25 kb upstream)	0.0024	1.6×10^{-17}	0.0025	2.8×10^{-10}	0.0024	2.3×10^{-25}
13	cg08160331	11q13.4	75,140,865	*KLHL35* (exon)	0.0032	2.8×10^{-18}	0.0028	7.9×10^{-10}	0.0027	7.9×10^{-20}
18	cg11751101	12p13.31	7,244,660	*C1R* (intron)	-0.0017	2.0×10^{-8}	-0.0027	4.0×10^{-11}	-0.0020	5.2×10^{-17}
6	cg04875128	15q13.3	31,775,895	*OTUD7A* (3' end)	0.0056	1.4×10^{-17}	0.0051	1.2×10^{-10}	0.0053	6.7×10^{-26}

Abbreviations: Chr, chromosome; *RASSF5*, Ras association domain family member 5; *MIR29B2*, microRNA 29b-2; *FHL2*, four and a half LIM domains 2; *SFMBT1*, Scm-like with four mbt domains 1; *TRIM59*, tripartite motif-containing 59; *CC2D2A*, coiled-coil and C2 domain containing 2A; *TRIM2*, tripartite motif containing 2; *SERINC5*, serine incorporator 5; *PCDHB1*, protocadherin beta 1; *ELOVL2*, elongation of very long chain fatty acids like 2; *ELOVL2-AS1*, ELOVL2 antisense RNA 1; *NHLRC1*, NHL repeat containing 1; *KLF14*, Kruppel-like factor 14; *KLHL35*, kelch-like 35; *C1R*, complement component 1, r subcomponent; *OTUD7A*, OTU domain containing 7A.

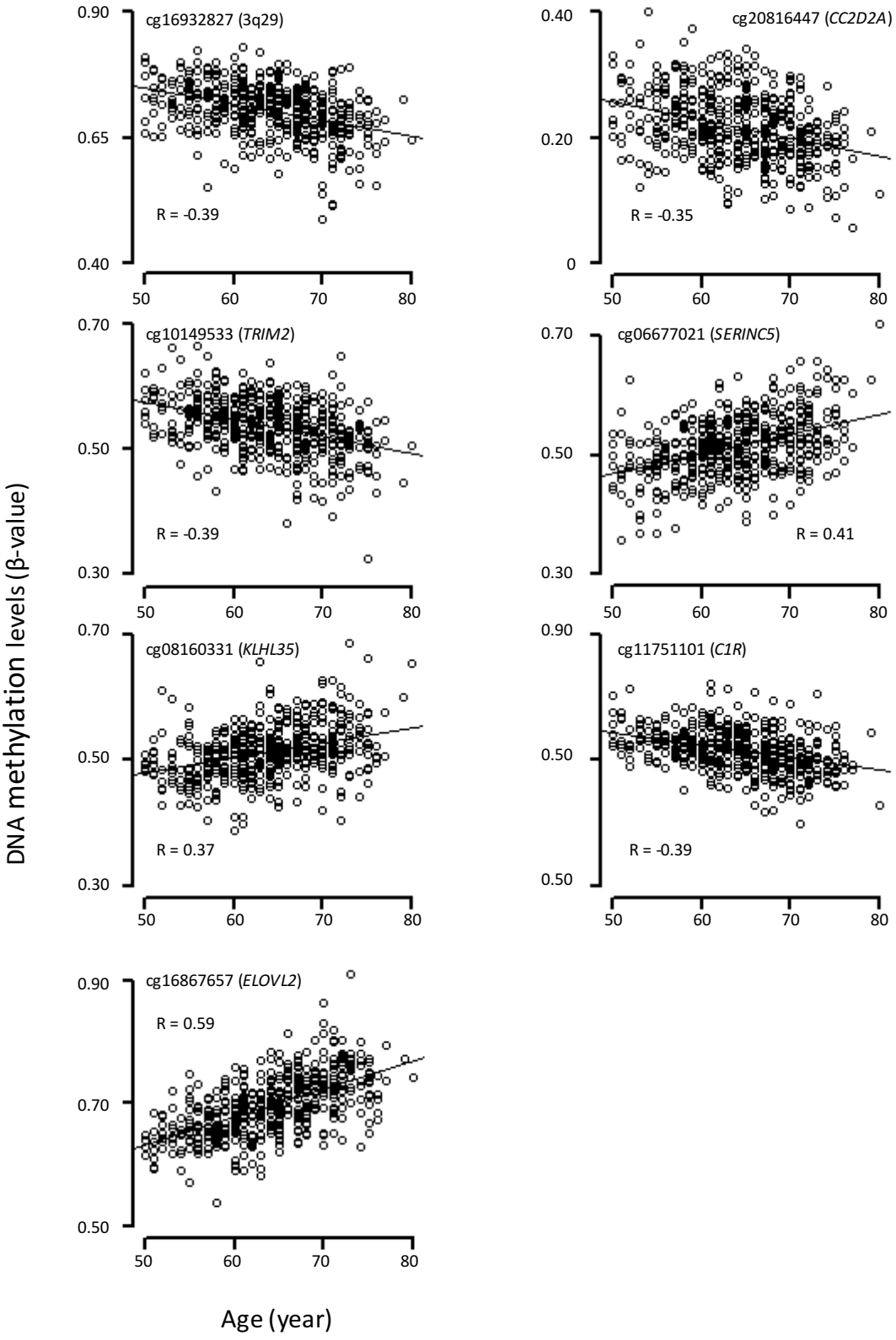

Figure 1 (1 of 3)

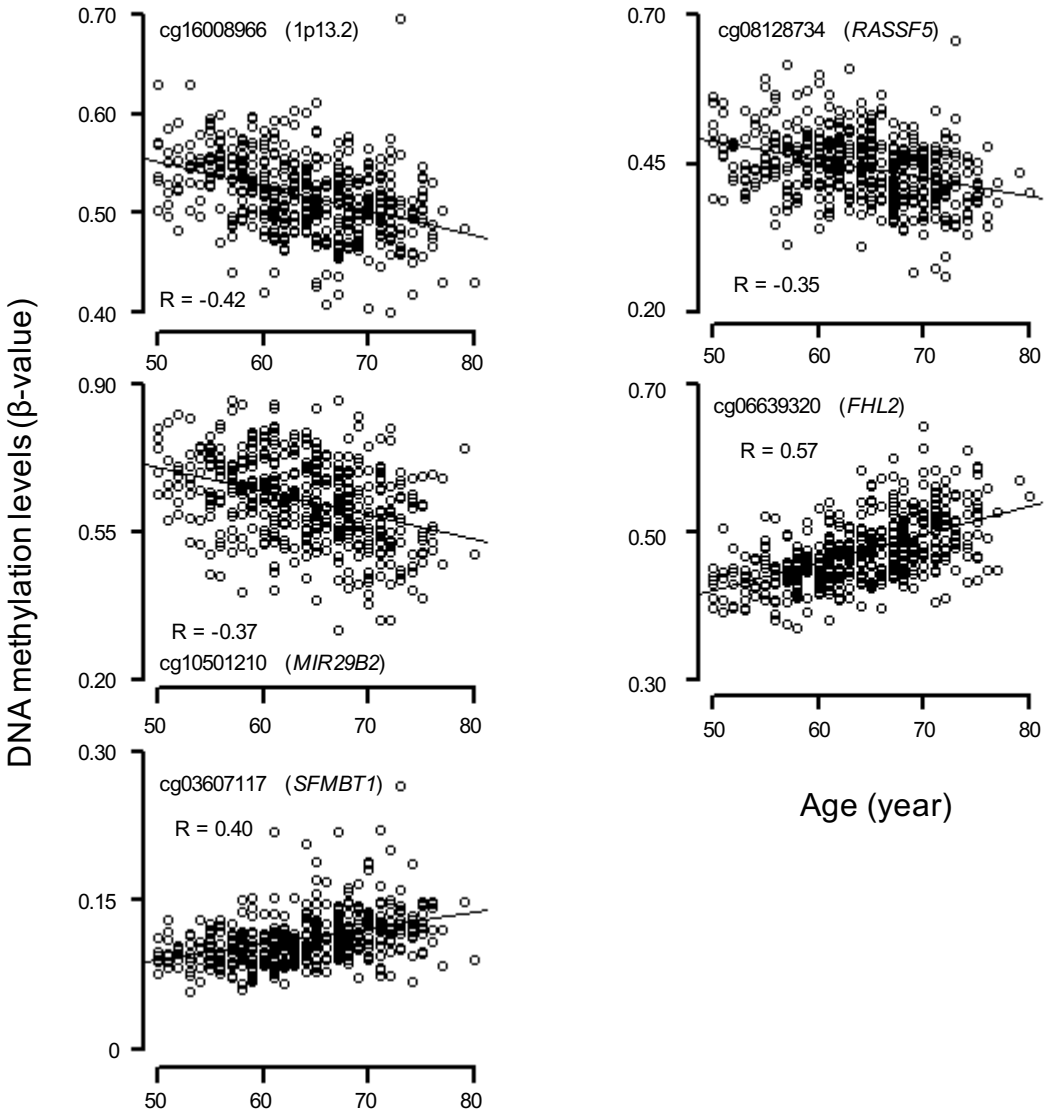

Figure 1 (2 of 3)

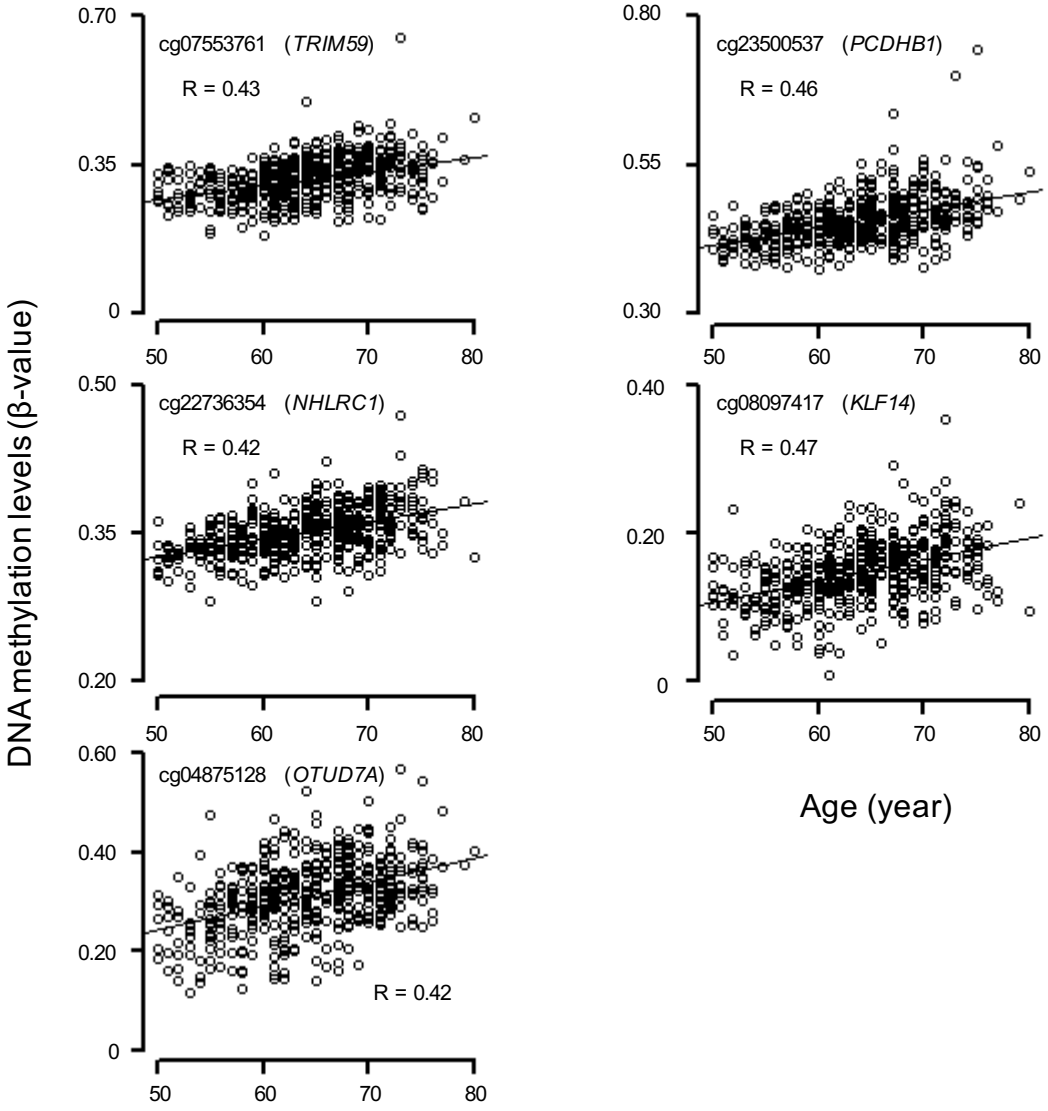

Figure 1 (3 of 3)

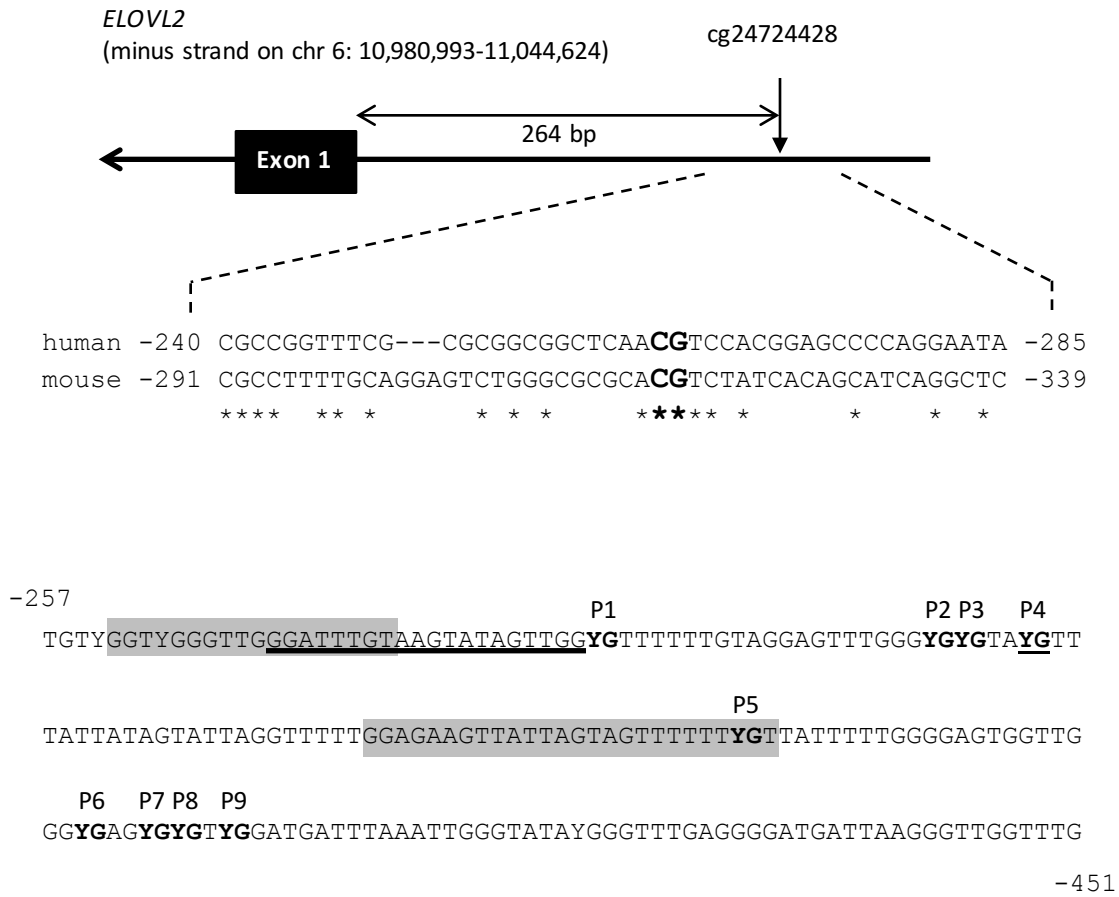
ELOVL2
(minus strand on chr 6: 10,980,993-11,044,624)
cg24724428
264 bp
Exon 1
human -240 CGCCGGTTTCG---CGCGGCGGCTCAACGTCCACGGAGCCCCAGGAATA -285
mouse -291 CGCCTTTTGCAGGAGTCTGGGCGCGCACGTCTATCACAGCATCAGGCTC -339
-257
P1
P2 P3 P4
TGTYGGTYGGGTTGGGATTTGTAAGTATAGTTGGYGTTTTTTGTAGGAGTTTGGGYGYGTAYGTT
P5
TATTATAGTATTAGGTTTTTGGAGAAGTTATTAGTAGTTTTTTYGTTATTTTTGGGGAGTGGTTG
P6 P7 P8 P9
GGYGAGYGYGTYGGATGATTTAAATTGGGTATAYGGGTTTGAGGGGATGATTAAGGGTTGGTTTG
-451

Figure 2

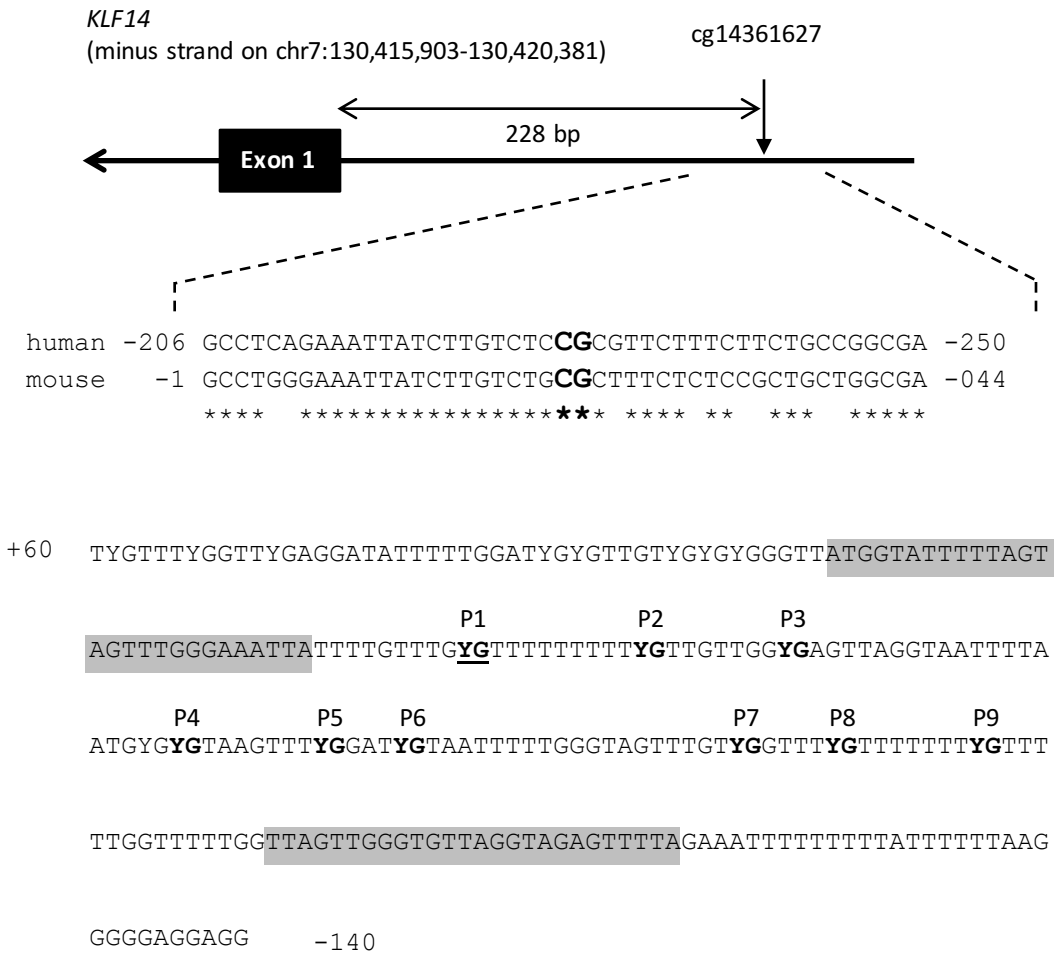
KLF14
(minus strand on chr7:130,415,903-130,420,381)
cg14361627
228 bp
Exon 1
human -206 GCCTCAGAAATTATCTTGTCTCCGCGTTCTTTCTTCTGCCGGCGA -250
mouse -1 GCCTGGGAAATTATCTTGTCTGCGCTTTCTCTCCGCTGCTGGCGA -044
+60 TYGTTTYGGTTYGAGGATATTTTTGGATYGYGTTGTYGYGYGGGTTATGGTATTTTTAGT
P1 P2 P3
AGTTTGGGAAATTATTTTGTTTGYGTTTTTTTTTYGTTGTTGGYGAGTTAGGTAATTTTA
P4 P5 P6 P7 P8 P9
ATGYGYGTAAGTTTYGGATYGTAATTTTTGGGTAGTTTGTYGGTTTYGTTTTTTTYGTTT
TTGGTTTTTGGTTAGTTGGGTGTTAGGTAGAGTTTTAGAAATTTTTTTTTATTTTTTAAG
GGGGAGGAGG -140

Figure 3

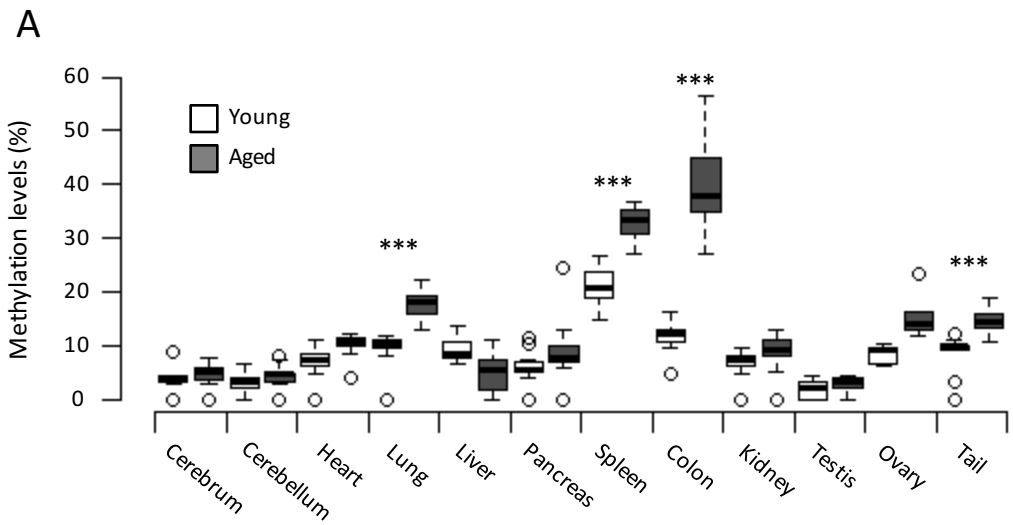
A
Methylation levels (%)
60
50
40
30
20
10
0
Young
Aged
***
***
***
***
Cerebrum
Cerebellum
Heart
Lung
Liver
Pancreas
Spleen
Colon
Kidney
Testis
Ovary
Tail

Figure 4 A

B

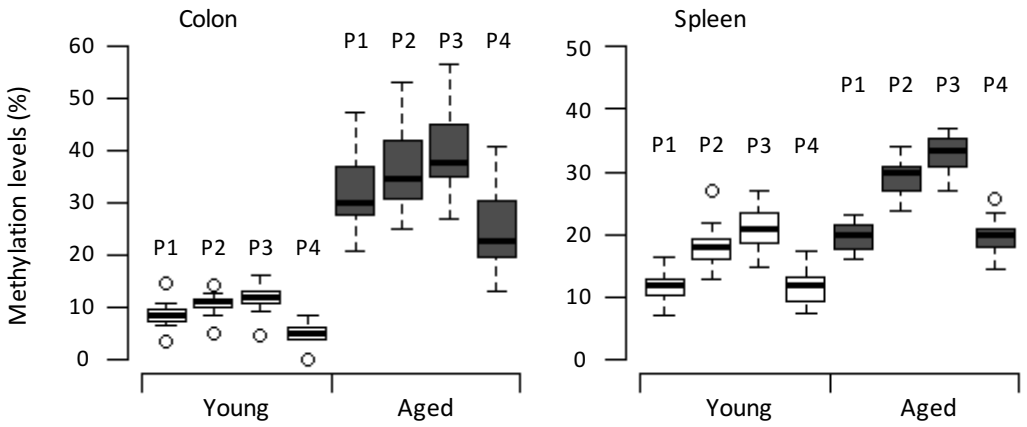
Colon
Spleen
Methylation levels (%)
0
10
20
30
40
50
60
P1
P2
P3
P4
Young
Aged

Figure 4 B

C

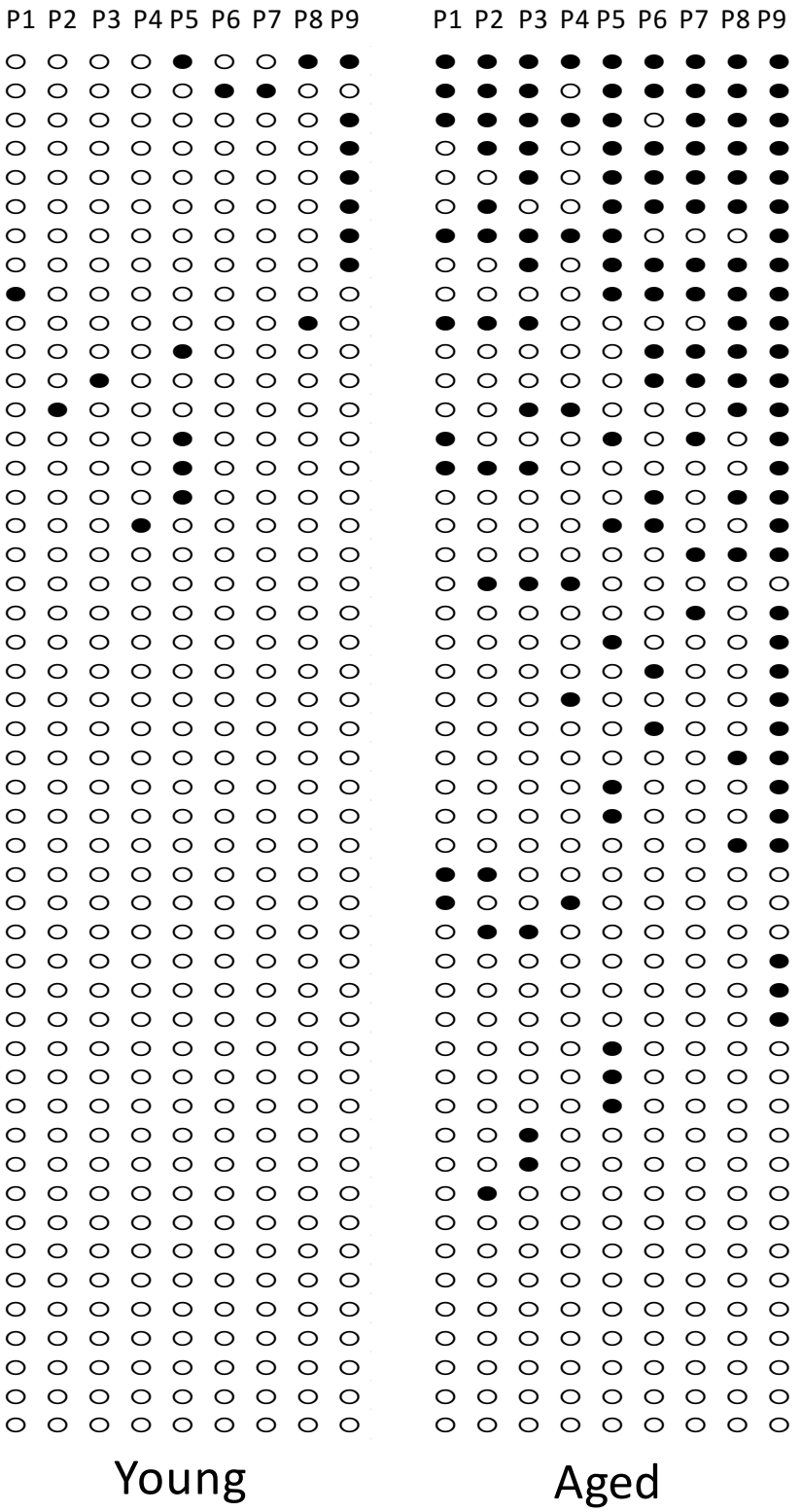

Figure 4 C

A

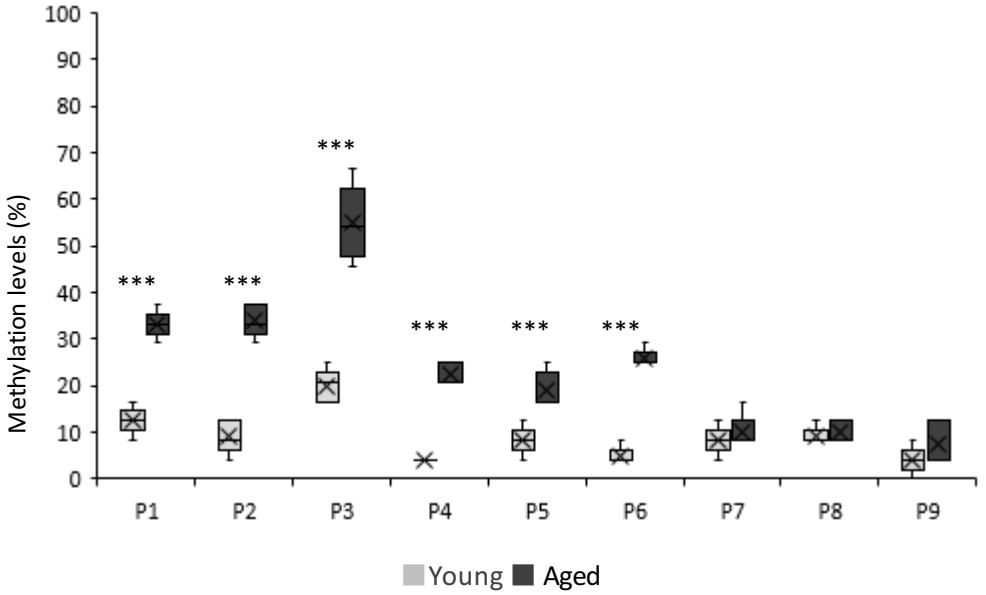

B

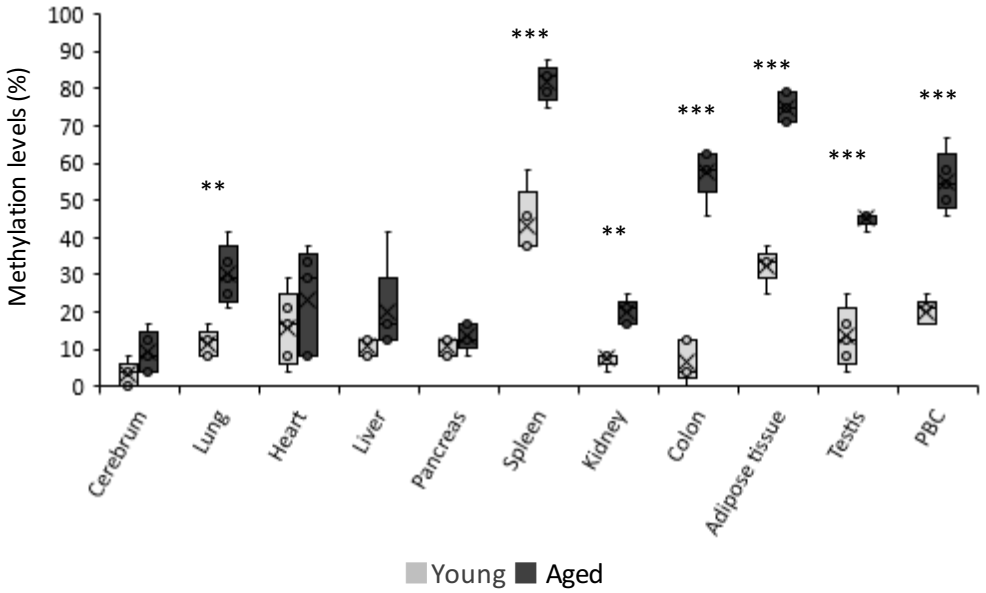

Figure 5 A and B

C

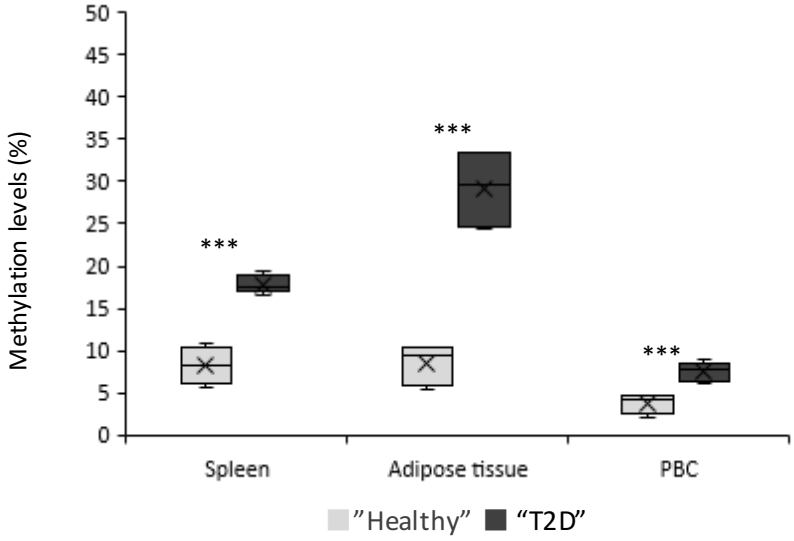

D

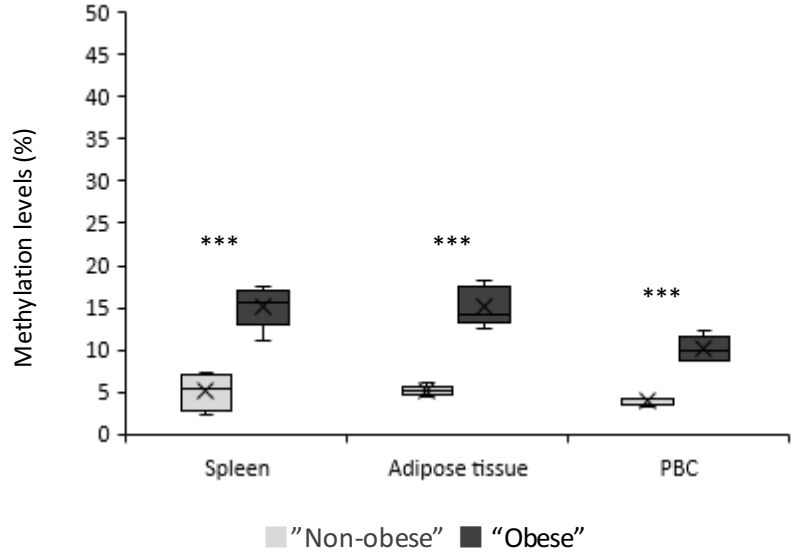

Figure 5 C and D

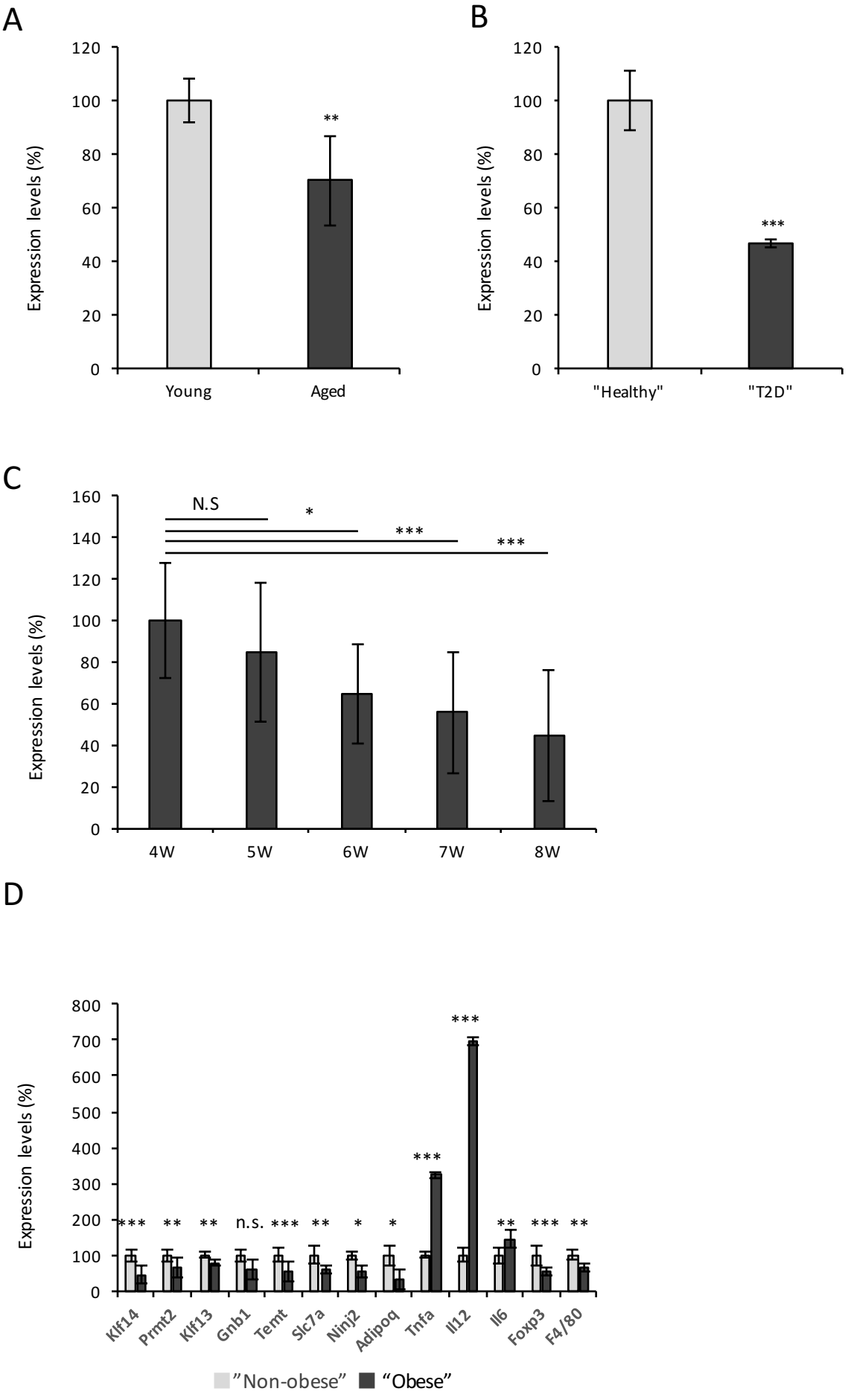
A
Expression levels (%)
120
100
80
60
40
20
0
**
Young
Aged
B
Expression levels (%)
120
100
80
60
40
20
0
***
"Healthy"
"T2D"
C
Expression levels (%)
160
140
120
100
80
60
40
20
0
N.S
*
***
***
4W
5W
6W
7W
8W
D
Expression levels (%)
800
700
600
500
400
300
200
100
0
***
***
**
**
n.s.
***
**
*
*
***
**
***
**
Klf14
Prmt2
Klf13
Gnb1
Temt
Slc7a
Ninj2
Adipoq
Tnfa
Il12
Il6
Foxp3
F4/80
"Non-obese"
"Obese"

Figure 6

A

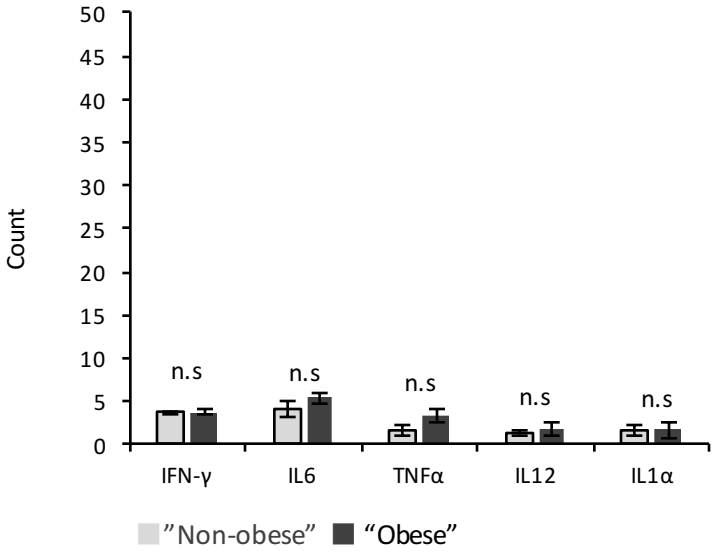
50
45
40
35
30
25
20
15
10
5
0
Count
n.s
n.s
n.s
n.s
n.s
IFN-γ
IL6
TNFα
IL12
IL1α
”Non-obese”
“Obese”

B

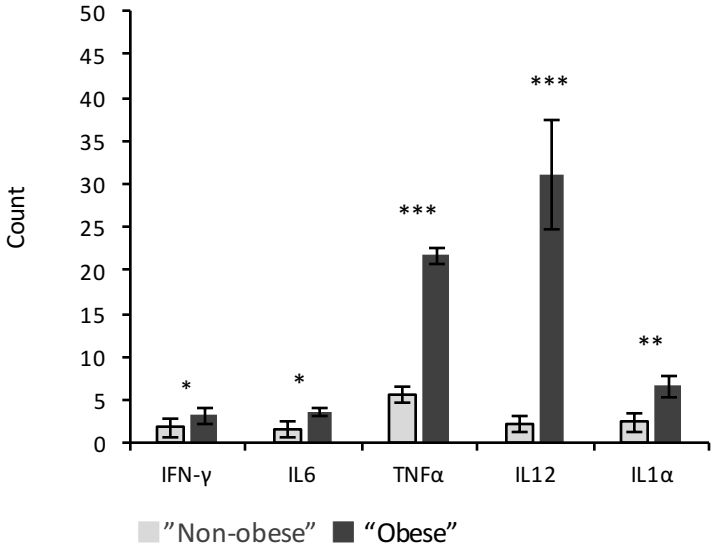
50
45
40
35
30
25
20
15
10
5
0
Count
*
*
***
***
**
IFN-γ
IL6
TNFα
IL12
IL1α
”Non-obese”
“Obese”

Figure 7

A

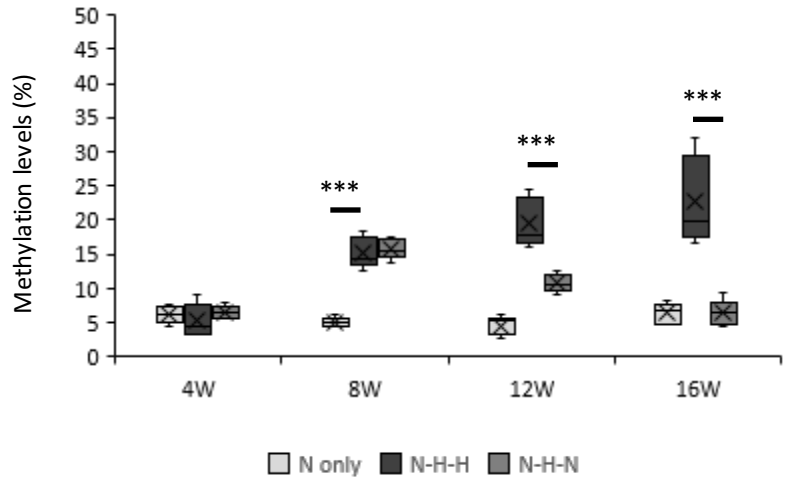
Methylation levels (%)
50
45
40
35
30
25
20
15
10
5
0
***
***
***
4W
8W
12W
16W
N only
N-H-H
N-H-N

B

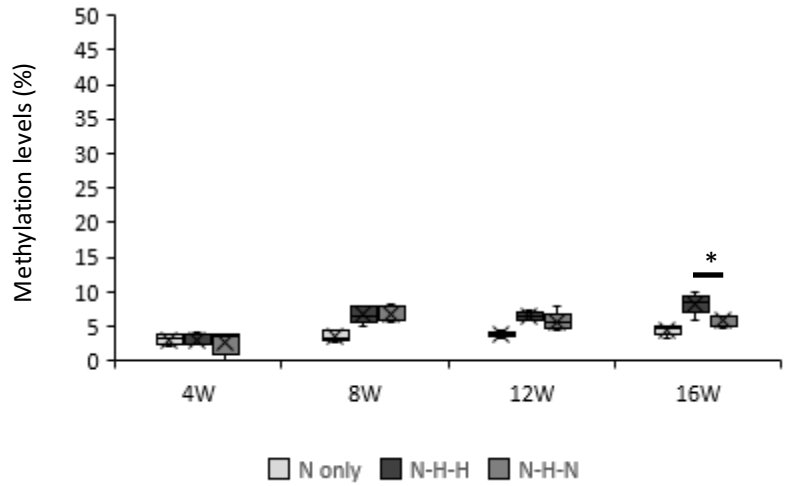
Methylation levels (%)
50
45
40
35
30
25
20
15
10
5
0
*
4W
8W
12W
16W
N only
N-H-H
N-H-N

Figure 8

Supplementary Table 1. Cohorts used in EWAS.

	Fukuoka Cohort Study		KING Study		Combined[a]	
Subjects (male/female)	287	(136/151)	192	(192/0)	479	(328/151)
Mean age, SD (year)	62.9	(6.4)	66.0	(6.0)	64.1	(6.4)
Mena BMI, SD (kg/m^2)	23.4	(3.1)	23.1	(2.5)	23.2	(2.9)
Hypertension[b] (%)	63.6	-	57.8	-	61.3	-
Diabetes mellitus (%)	10.5	-	0.0	-	6.3	-
Dyslipidemia (%)	61.7	-	35.9	-	51.4	-

[a] The subjects of Kyushu University Fukuoka Cohort Study and the subjects of KING Study were combined.
[b] There was one missing value in the Fukuoka Cohort Study.

Supplementary Table 2: Summary of organs used.

		Cerebrum	Cerebellum	Heart	Lung	Liver	Pancreas	Spleen	Kidney	Colon	Testis / ovary	Tail	Adipose tissue	PBC
Elovl2	"Young" vs "Aged"	◯	◯	◯	◯	◯	◯	◯	◯	◯	◯	◯	×	×
Fhl2	"Young" vs "Aged"	◯	◯	◯	◯	◯	◯	◯	◯	◯	◯	◯	×	×
Trim59	"Young" vs "Aged"	◯	◯	◯	◯	◯	◯	◯	◯	◯	◯	◯	×	×
Klf14	"Young" vs "Aged"	◯	×	◯	◯	◯	◯	◯	◯	◯	◯	×	◯	◯
	"Healthy" vs "T2D"	×	×	×	×	×	×	◯	×	×	×	×	◯	◯
	"Non-obese" vs "Obese"	×	×	×	×	×	×	◯	×	×	×	×	◯	◯

Supplementary Table 3.
Primers for quantitative reverse transcription PCR.

Gene		Primer sequence (5′ – 3′)
Il1a	F	TGGTTAAATGACCTGCAACAGGAA
	R	AGGTCGGTCTCACTACCTGTGATG
Il6	F	CCACTTCACAAGTCGGAGGCTTA
	R	CCAGTTTGGTAGCATCCATCATTTC
Adipoq	F	TTCTGTCTGTACGATTGTCAGTGGA
	R	GGCATGACTGGGCAGGATTA
Tnf	F	ACTCCAGGCGGTGCCTATGT
	R	GTGAGGGTCTGGGCCATAGAA
Il12a	F	CCGGTCCAGCATGTGTCAA
	R	CAGGTTTCGGGACTGGCTAAGA
Klf14	F	AGCCTGCAGGAACCTTTGAGAA
	R	GGTGAGACACCAGAGTCATTTGGA
Actb	F	CATCCGTAAAGACCTCTATGCCAAC
	R	ATGGAGCCACCGATCCACA
Slc7a10	F	AGCGGGTGGCACTCAAGAA
	R	GACACCCTTGGGTGAGATGAAGA
Aph1c	F	TGCTCATCTTCGGAGCGTTG
	R	CAGTCGCATCGAGGGTGCTA
Gnb1	F	TTGCTGGGTATGATGACTTCAACTG
	R	TGACTCGGTTGTCGTGTCCA
Klf13	F	GTTTACGGGAAATCTTCGCACCT
	R	CGTGCGAACTTCTTGTTGCACT
Ninj2	F	CAGGACCTCCAGCAATCCTA
	R	TTAATTCTGGTGCTGTGGACAA
Prmt2	F	TGCAGAATGGCTTTGCTGAC
	R	GGAAACATAGGCGAGAACTTGG
Tpmt	F	AAGAGCACCCTGATGCTGAGGTA
	R	CGCAGTCCACTCTGGCCTTTA

Supplementary Figure 1

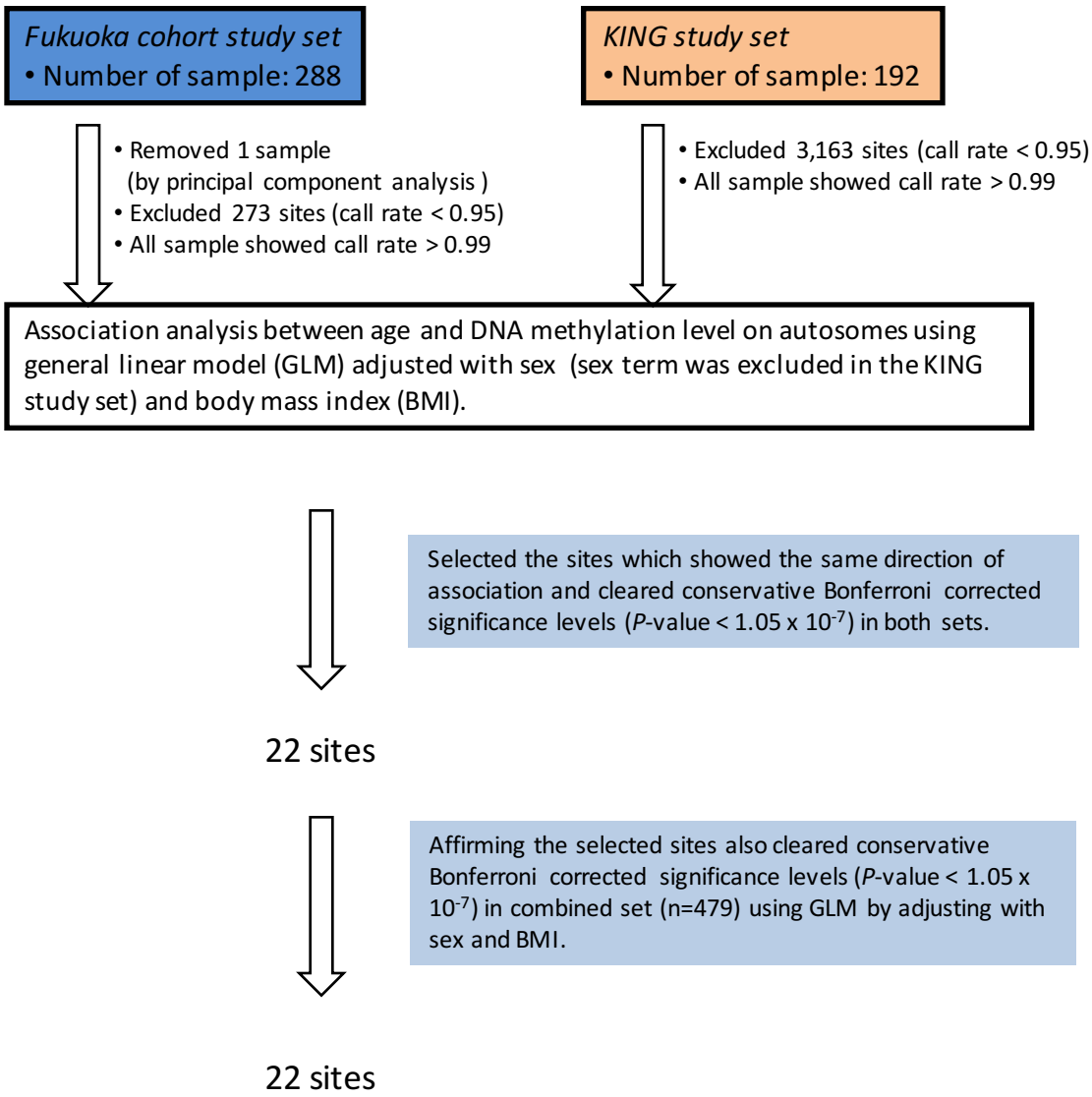

Supplementary Figure 1.
Flow chart summarizing the design for identification of CpG sites associated with age. Bonferroni correction was done using a total number of CpG site (473,864) on autosomes.

Supplementary Figure 2

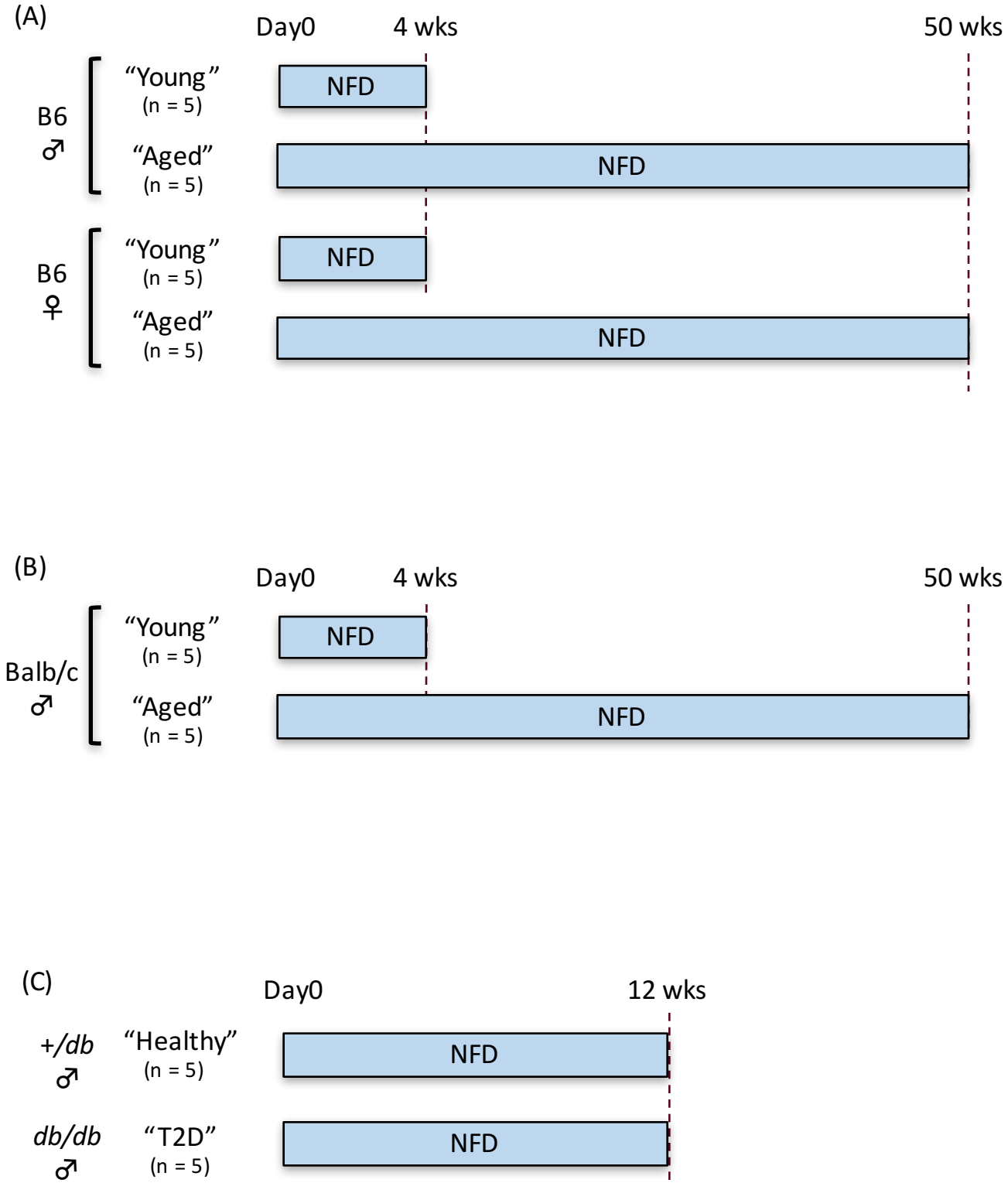

Supplementary Figure 2

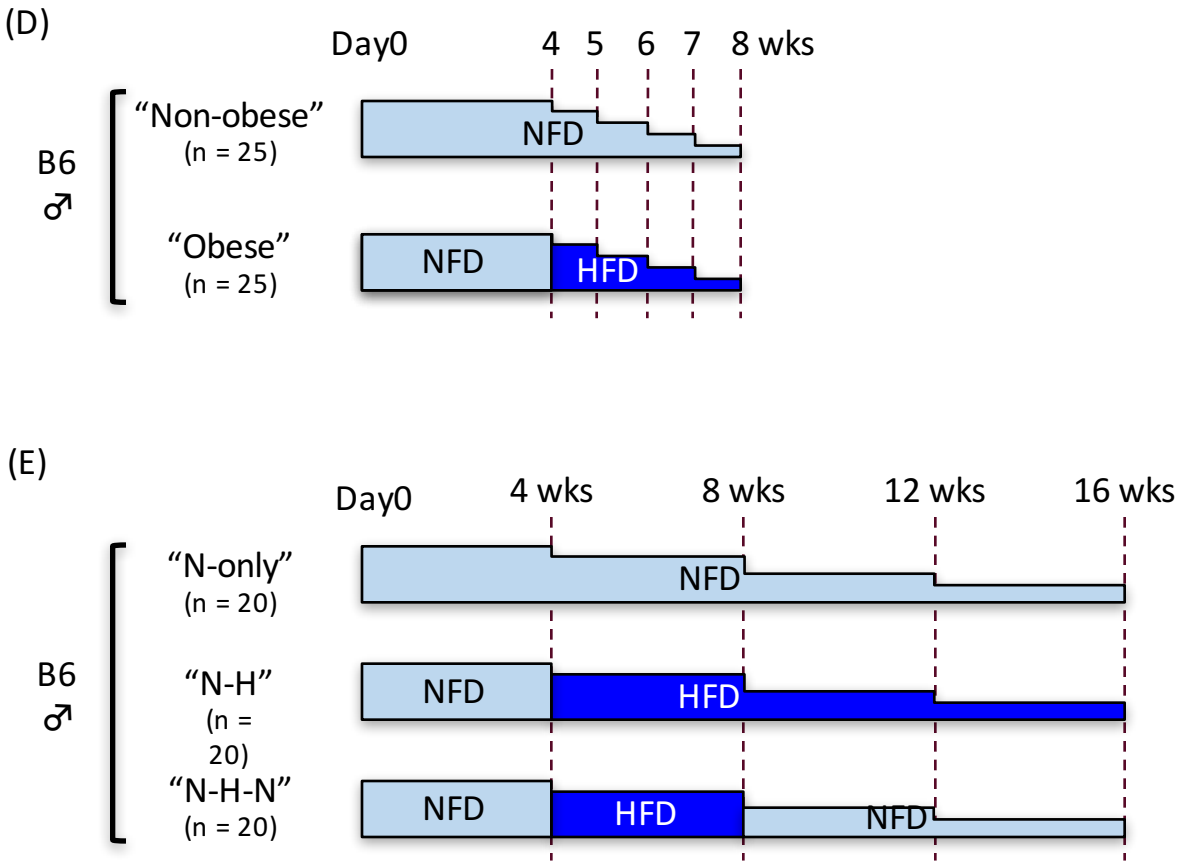

Supplementary Figure 2.
The schematic diagram of treatments of mice. NFD: normal fat diet. HFD: high fat diet. (A) The scheme for treatment of the "Young" and "Aged" B6 mice. I dissected 4 week-old and 50 week-old mice as the "Young and "Aged" groups, respectively. I prepared diet-matched 5 males and 5 females for each treatment. (B) The scheme for treatment of the "Young" and "Aged" Balb/c mice. (C) The scheme for treatment of the "T2D" and "Healthy" mice matched for age, sex and diet. I used 12 week-old homozygous *db*/*db* mice and heterozygous +/*db* mice as "T2D" and "Healthy" mice, respectively. (C) The scheme for treatment of the "Non-obese" and "Obese" mice. I raised male B6 mice (n = 50) for 4 weeks then switched into HFD only for 25 mice as the "Obese" group while I kept raising the remaining 25 with NFD as the "Non-obese" group. I sacrificed 5 mice from each treatment every week to collect 4, 5, 6, 7 and 8 week-old mice in two different diets. (D) The scheme for treatment of three different dietary conditions. I raised 5 male B6 mice with only NFD for 12 weeks as the "N-only" (NFD-only) group. I also raised another 5 male B6 mice with NFD for 4 weeks then switched to HFD for 8 weeks as the "N-H" (NFD-HFD) group. In addition, another 5 male B6 mice with NFD for 4 weeks then switched to HFD for 4 weeks then switched back to NFD for 4 weeks as the "N-H-N" (NFD-HFD-NFD) group.

Supplementary Figure 3

A

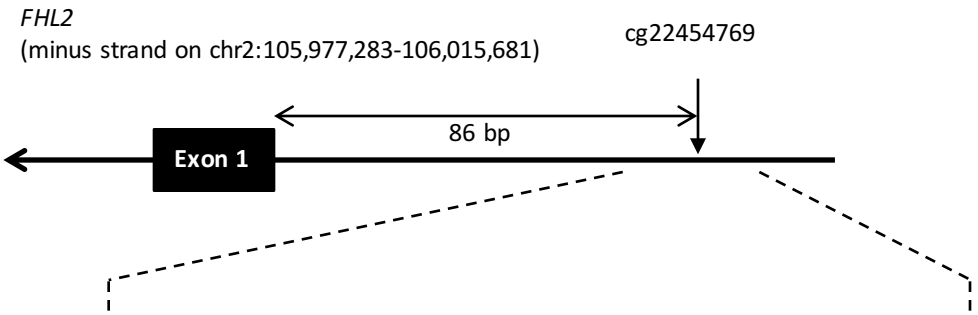


```
human -58  CGGGAGCGTCGCCTCCGGCGTGGGCTCTCGGGCGCGAGTTTCGGACGAG -106
mouse +549 CAACCCTCGCTGCGTCCTGGCCTTGGCTCCAGGGCTAGTTGCTATGCAG +501
           *        *  *  *   *      * *     ** **** *
```

```
                                                        P1      P2      P3
+99   TGTGGTGGGGTTGGGGTTTAAGGGAATTTAGTGGATTGTGGATYGGTGGYGGTGGYGGTT
          P4   P5                    P6          P7          P8
      TAGYGGGYGGAGTGTAGTAGGAGTTGYGTTYGTTTTYGAGAATTTTYGTTGAGTTATTTG
                        P9
      ATTATATAAGGATATAYGYGTTYGGGYGGYGGGTTGGGYGYGTTGGTTAGGAGAGTTAGG

      YGTGGTAGYGAGYGTTTTTYGGTAGTTAGTYGGTTGTYGTTTGTTTTTTTGATGAYGTTA

      TTATAGATTTTTTGTTTGATTTAATTTTTTTTTTTGTTTTTTGGTGTTTGGTTTATAYGG

      TTAATTTTYGTTGYGTTTTGGTTTTGGTTTTAGGGTTAGTTGTTATGTAGTGTAGAGAGT

      TGTAGTAGTTGATATTTAAGGGYGAAATGATATGGGGTTATTGTTATTAGGATAYGTTTG

      GGTTGYGGGGTTTTGTTTGAGTGTAGTTTGGTGTAAGTATGGATGGGTTATTTGTAGATT

      TGGGGGAAGGAATTATGTGT     -522
```

Supplementary Fig. 3A.
The age-associated methylation site, cg22454769, in the promoter region of *FHL2*. There are 28 CpG sites located in the mouse target region of *Fhl2*. However, the CpG site corresponding to cg22454769 was substituted by CC in mouse.

Supplementary Figure 3

B

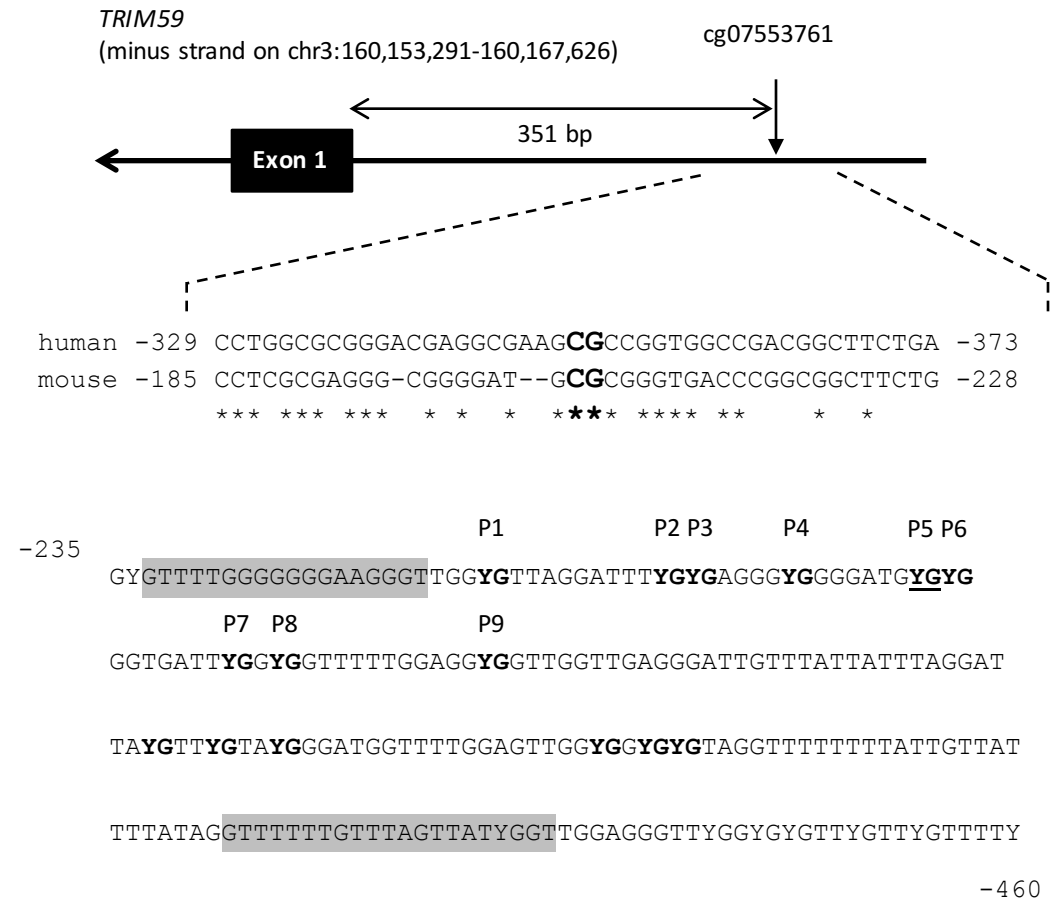

Supplementary Fig. 3B.
The age-associated methylation site, cg07553761, in the promoter region of *TRIM59*. There are 15 CpG sites located in the mouse target region of *Trim59*. P5 is the site corresponding to cg07553761 in human.

Supplementary Figure 4

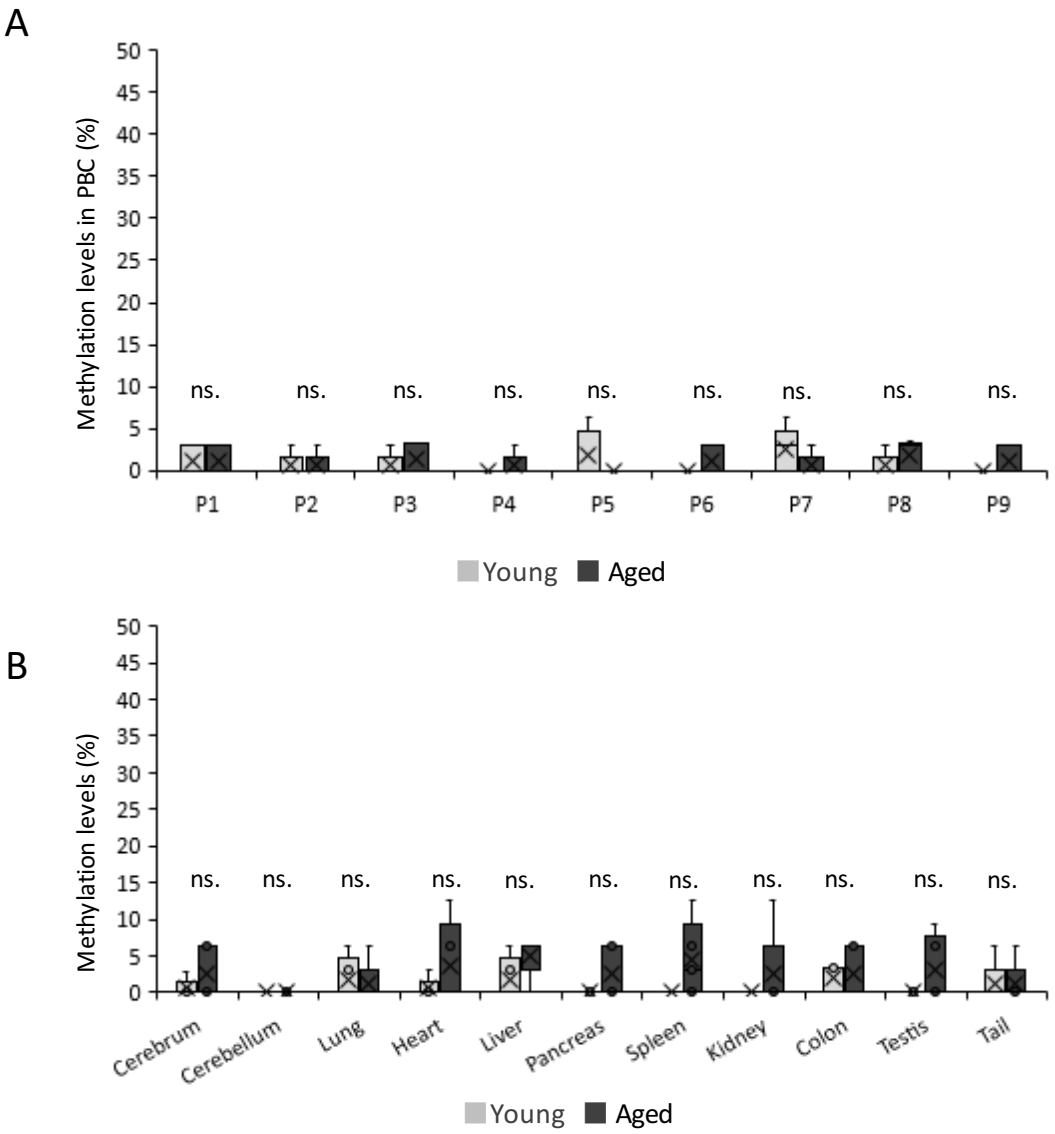

Supplementary Figure 4.
DNA methylation levels in *Fhl2* compared between the "Young" and "Aged" mice. (A) The methylation levels at multiple CpG sites (P1-P9) in *Fhl2* in the spleen compared between diet-matched "Young" and "Aged" male B6 mice. (B) The methylation levels at P3 in *Fhl2* in various organs compared between diet-matched "Young" and "Aged" male B6 mice. Five mice were used in each group (**P* < 0.05, ***P* < 0.01, ****P* < 0.005. Error bars represent means ± SD).

Supplementary Figure 5

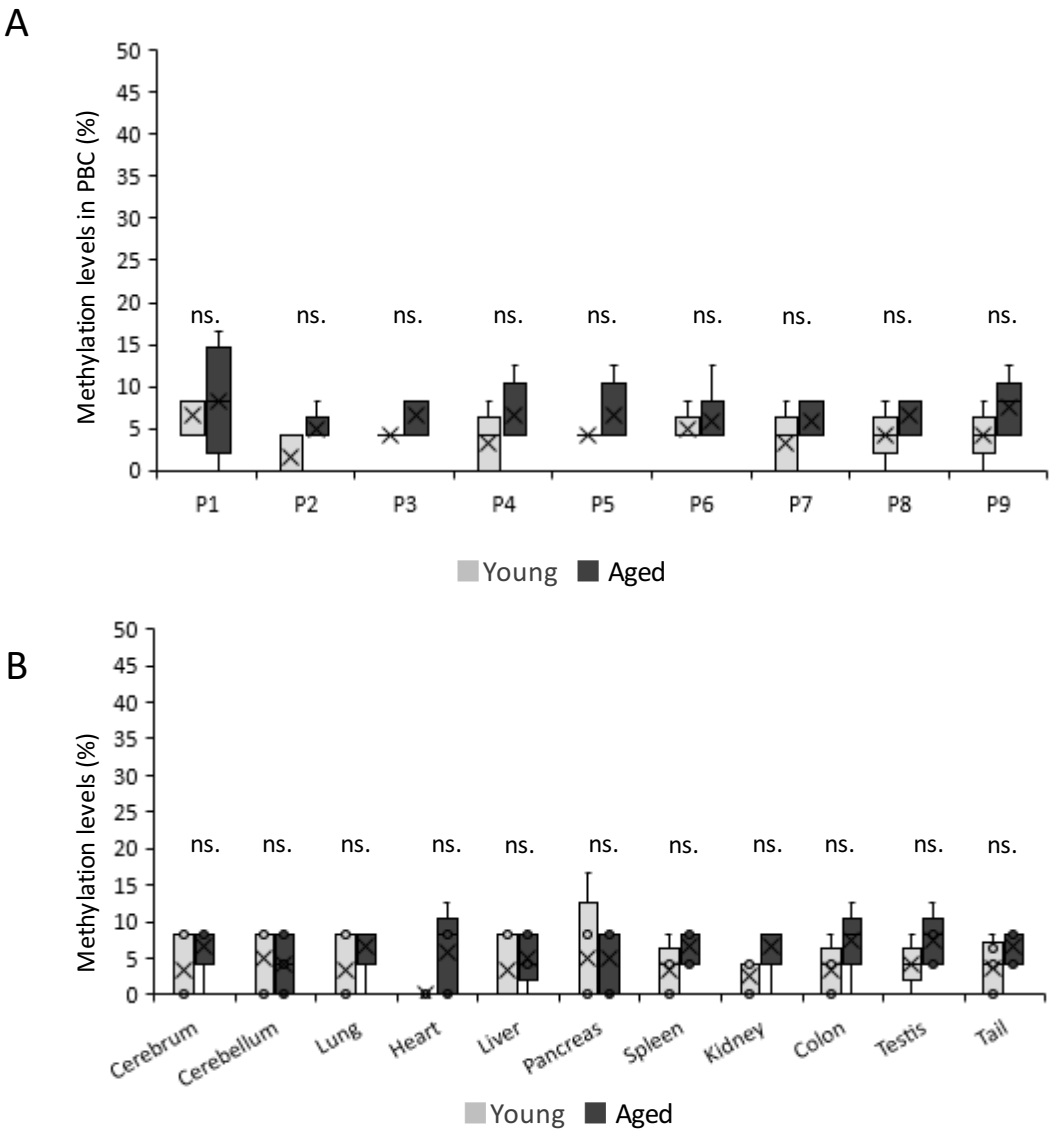

Supplementary Figure 5.
DNA methylation levels in *Trim59* compared between the "Young" and "Aged" mice. (A) The methylation levels at multiple CpG sites (P1-P9) in *Trim59* in the spleen compared between diet-matched "Young" and "Aged" male B6 mice. (B) The methylation levels at P5 in Trim59 in various organs compared between diet-matched "Young" and "Aged" male B6 mice. Five mice were used in each group (*$P < 0.05$, **$P < 0.01$, ***$P < 0.005$. Error bars represent means ± SD).

Supplementary Figure 6

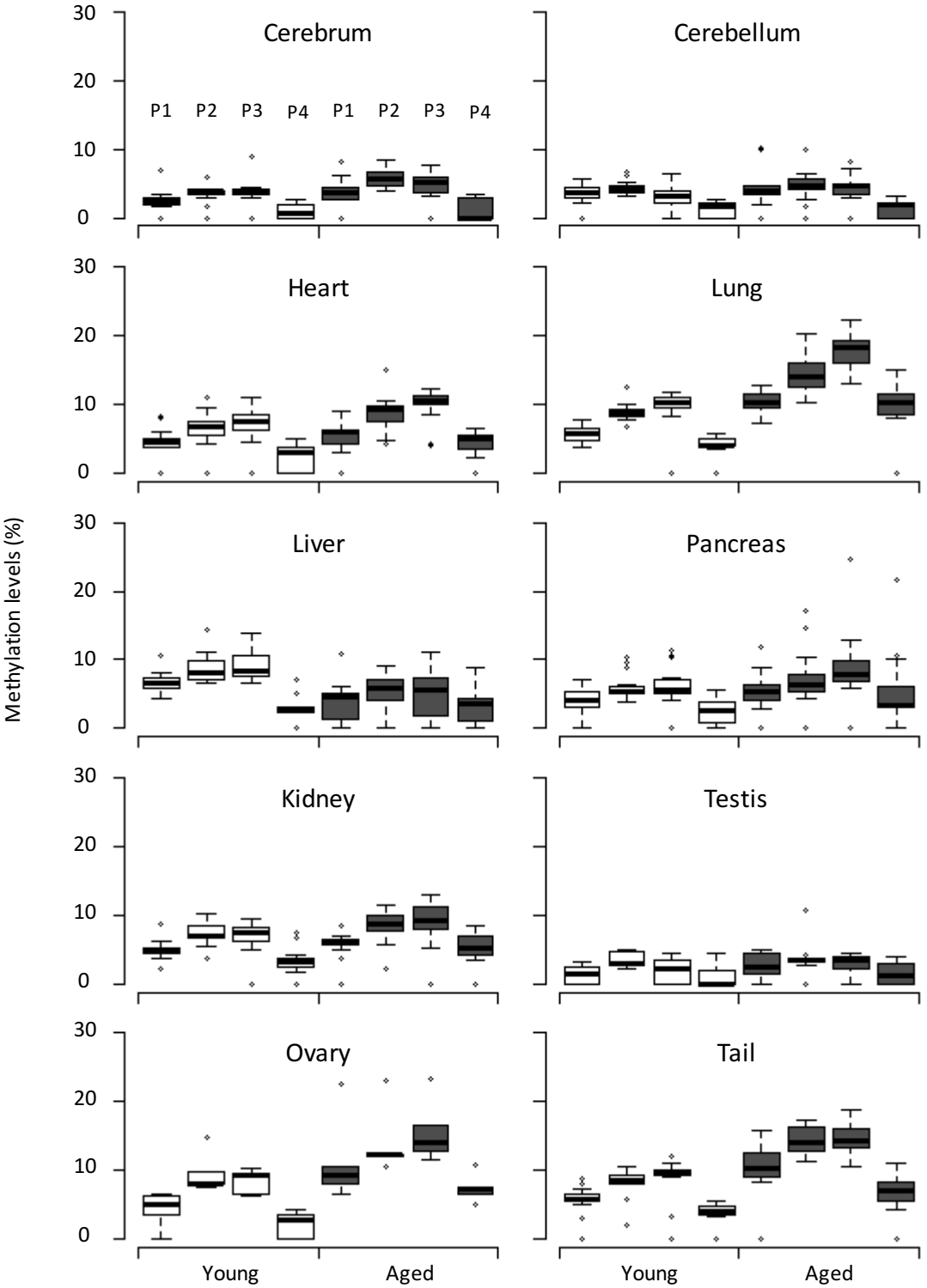

Supplementary Figure 6.
DNA methylation levels at P1-P4 in *Elovl2* in other organs from "Young" and "Aged" mice.

Supplementary Figure 7

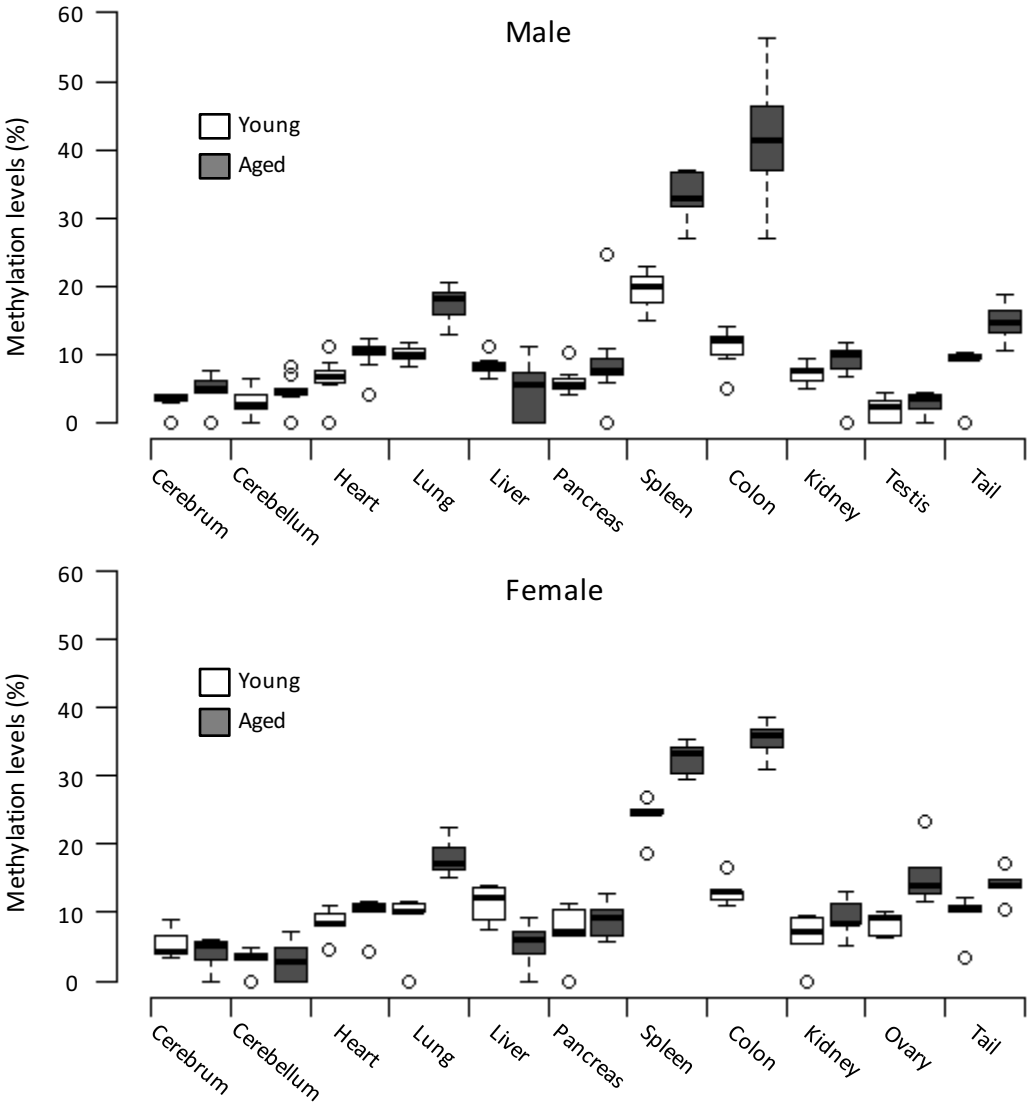

Supplementary Figure 7.
DNA methylation levels at P3 in *Elovl2* were not different between male and female mice in various organs.

Supplementary Figure 8

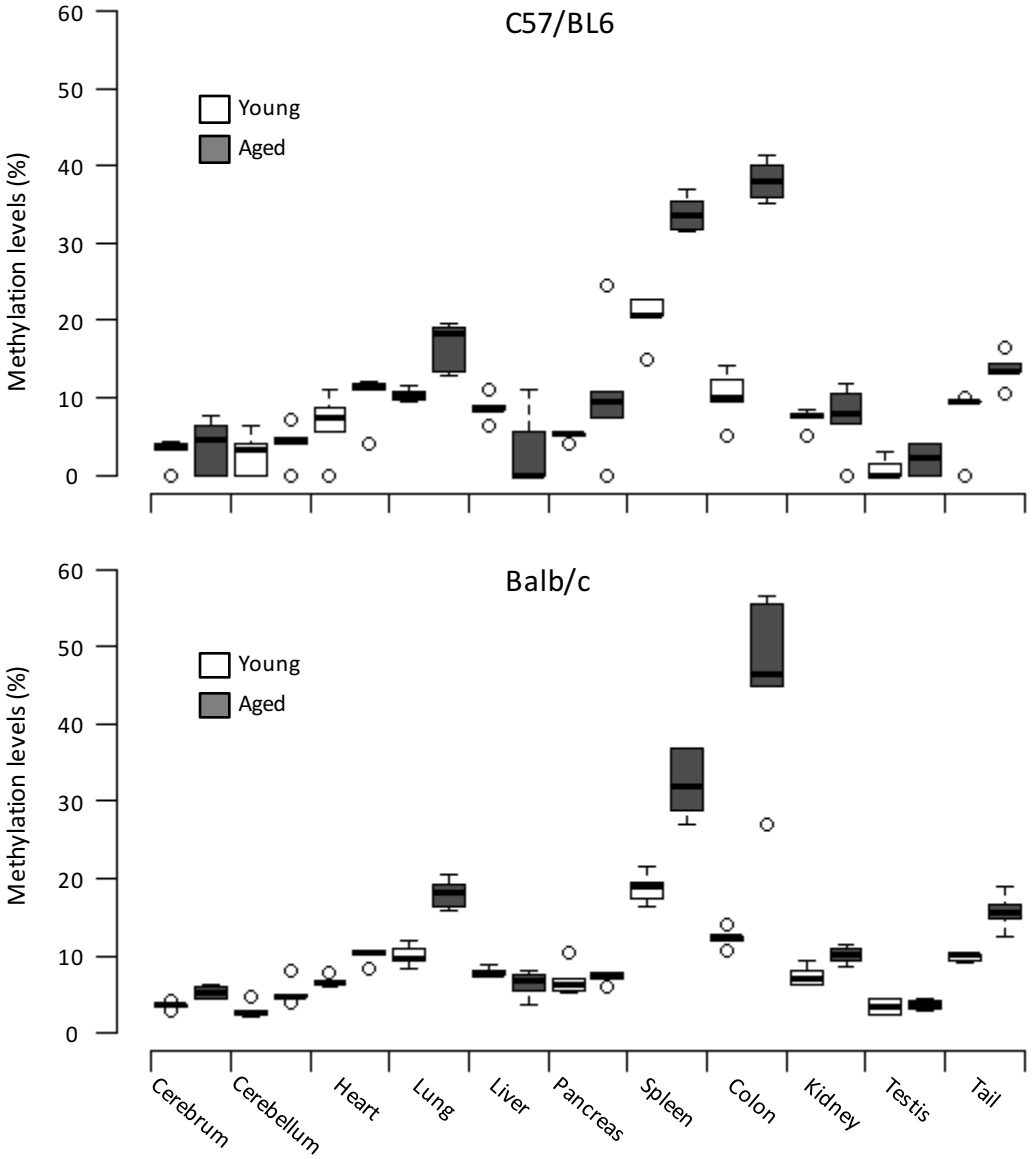

Supplementary Figure 8.
DNA methylation levels at P3 in *Elovl2* were not different between C57/B6 and Balb/c mice in various organs. Only the methylation levels of male mice were blotted.

Supplementary Figure 9

A

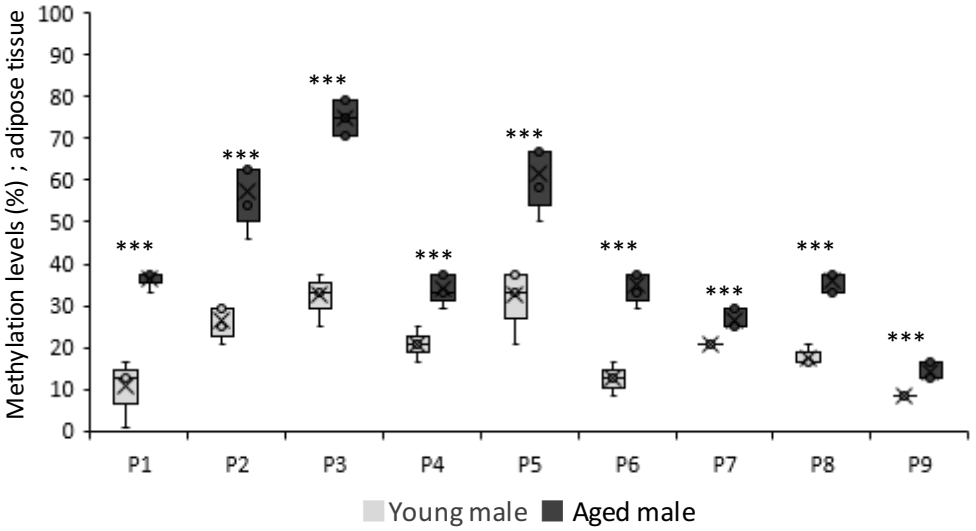

B

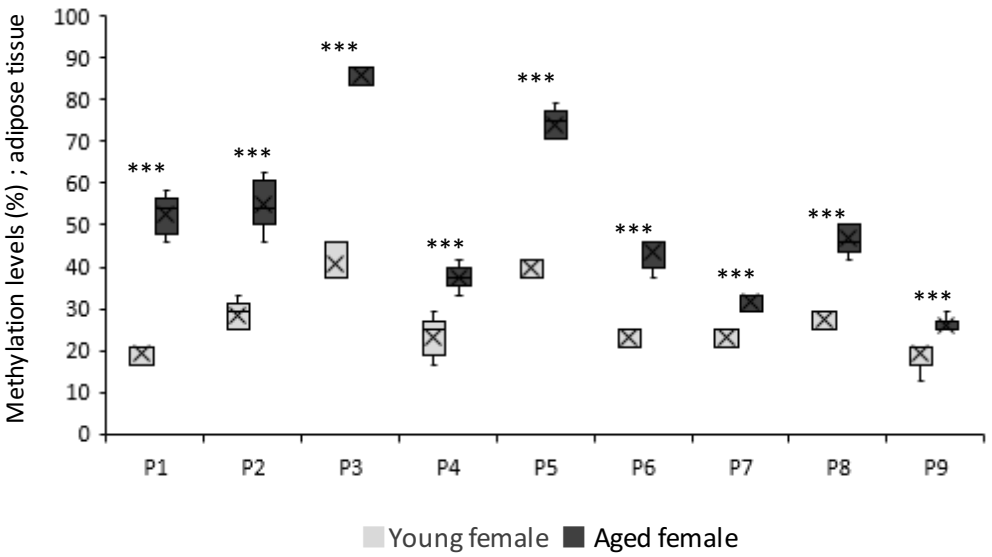

Supplementary Figure 9

C

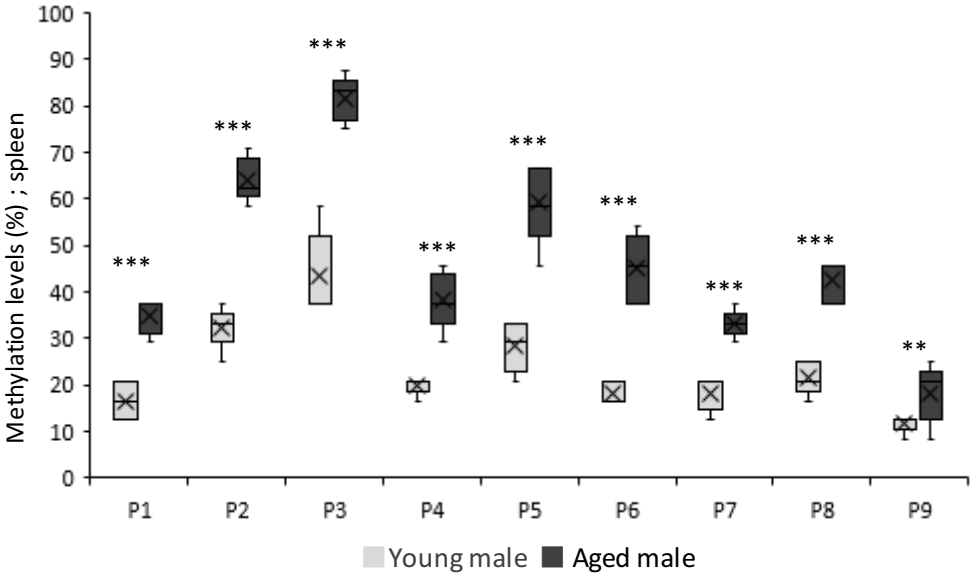

D

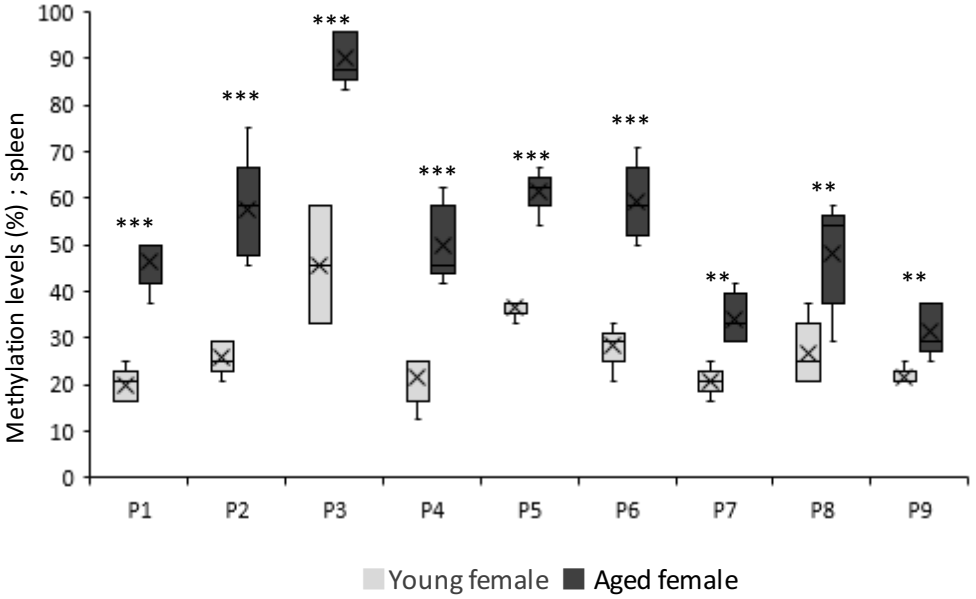

Supplementary Figure 9.
DNA methylation levels at P3 in *Klf14* compared between the "Young" and "Aged" mice in male adipose tissue (A), female adipose tissue (B), male spleen (C) and female spleen (D). Five mice were used in each group (*$P < 0.05$, **$P < 0.01$, ***$P < 0.005$. Error bars represent means ± SD).

Supplementary Figure 10

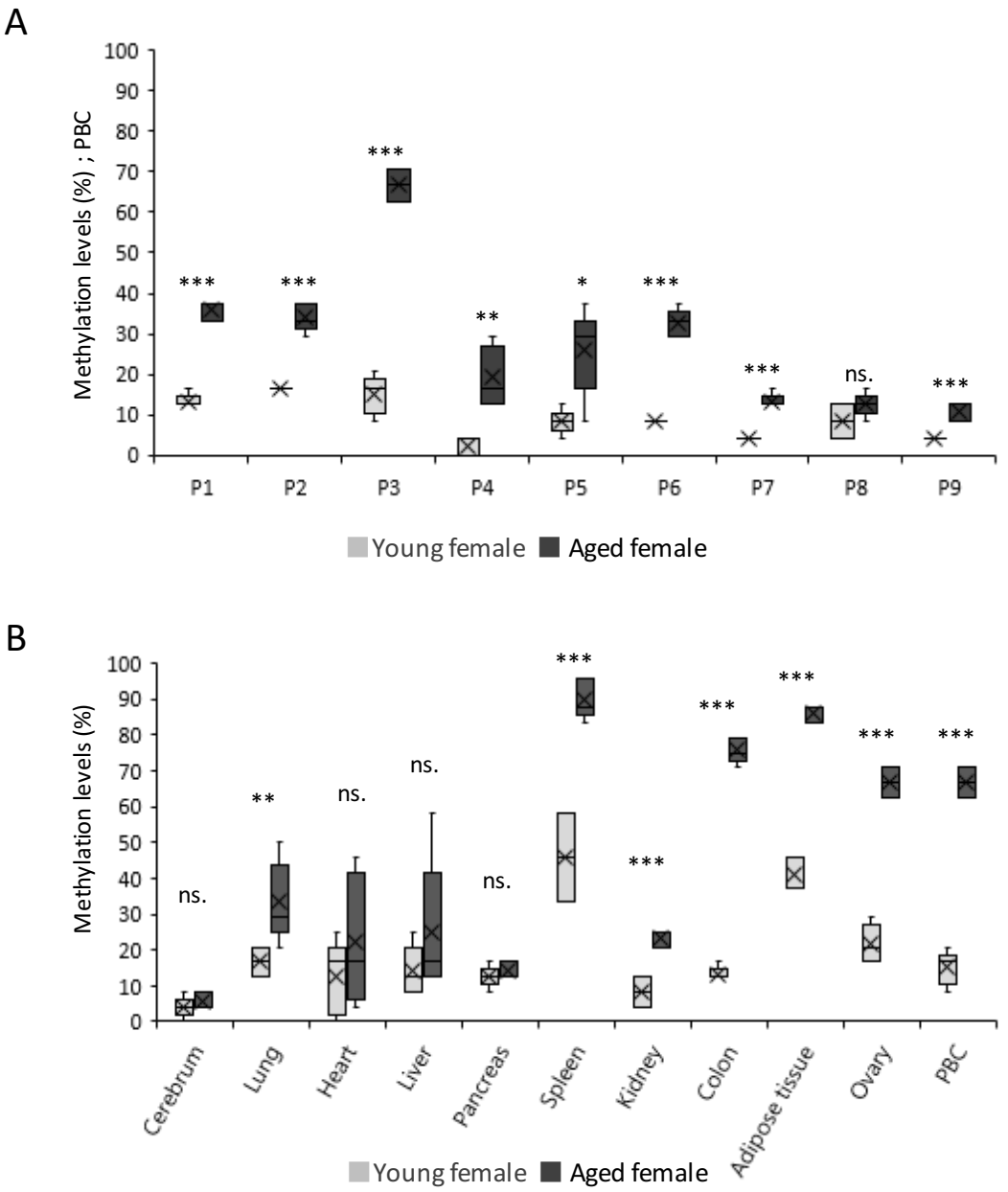

Supplementary Figure 10 .
DNA methylation levels in *Klf14* compared between the "Young" and "Aged" mice. (A) DNA methylation levels at 9 CpG sites in *Klf14* in the PBC compared between the "Young" and "Aged" female mice. Five mice were used in each group (**P* < 0.05, ***P* < 0.01, ****P* < 0.005. Error bars represent means ± SD).

Supplementary Figure 11

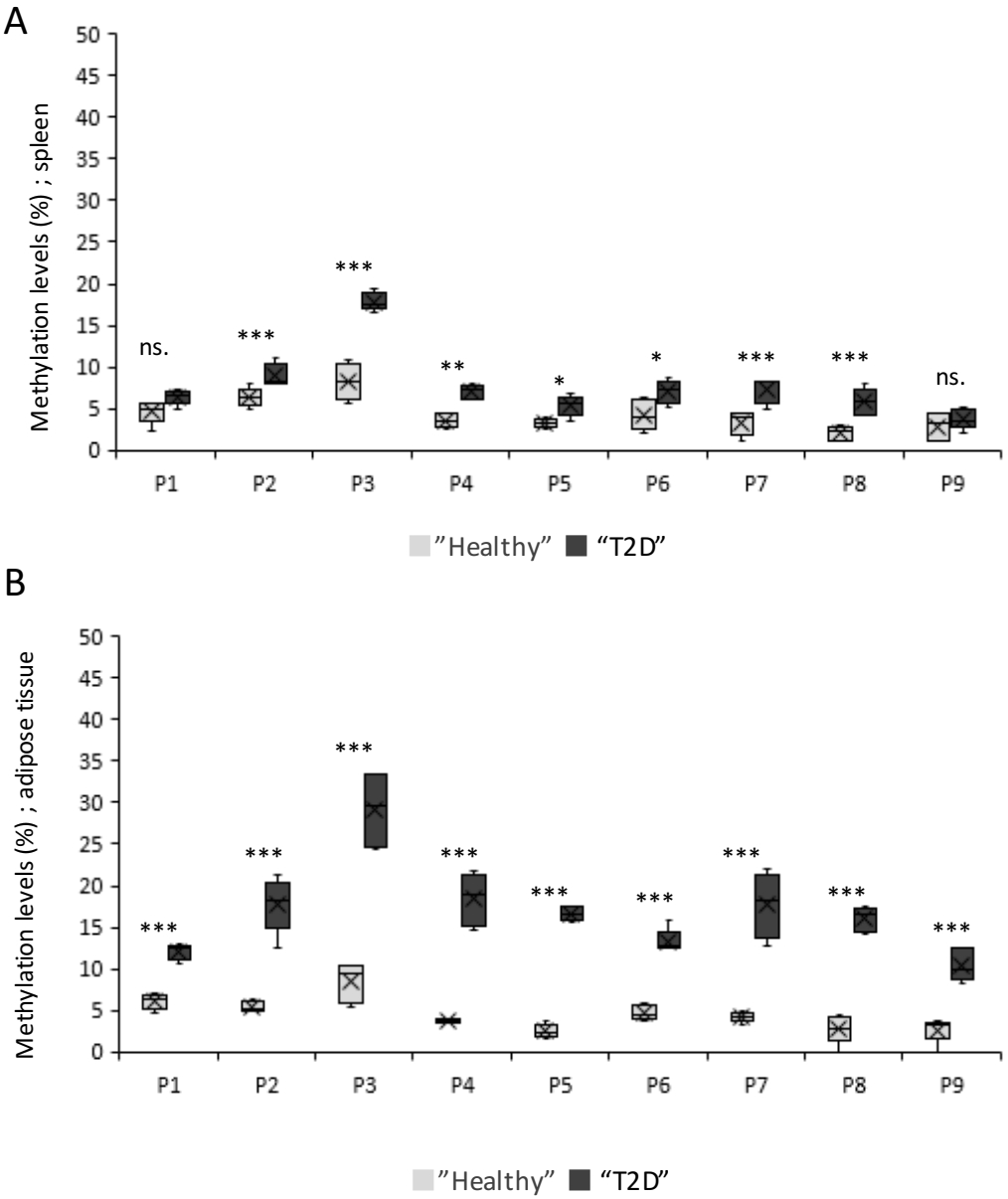

Supplementary Figure 11

C

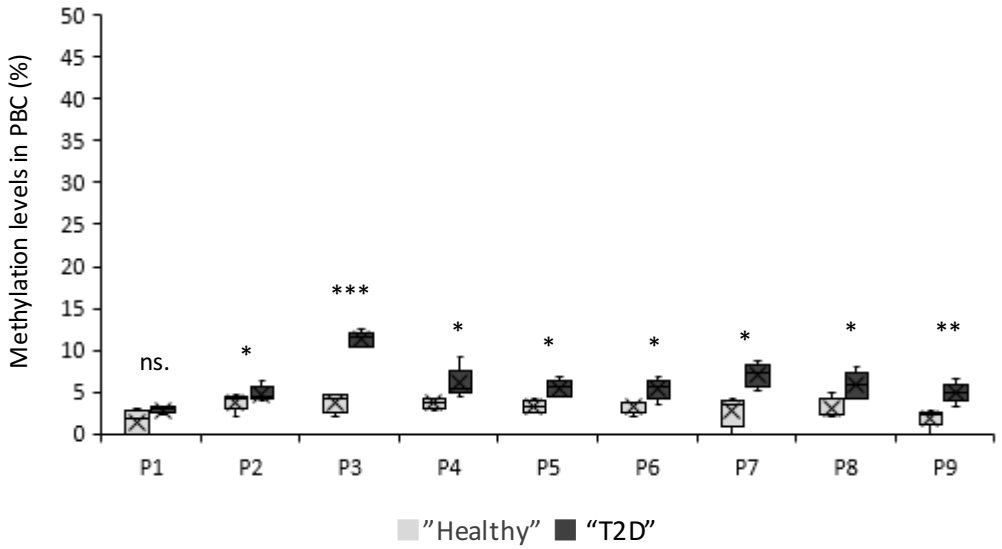

Supplementary Figure 11.
DNA methylation levels at 9 CpG sites in *Klf14* compared between the "Healthy" and "T2D" mice. in the spleen (A), the adipose tissue (B) and PBC (C). Five mice were used in each group (**P* < 0.05, ***P* < 0.01, ****P* < 0.005. Error bars represent means ± SD).

Supplementary Figure 12

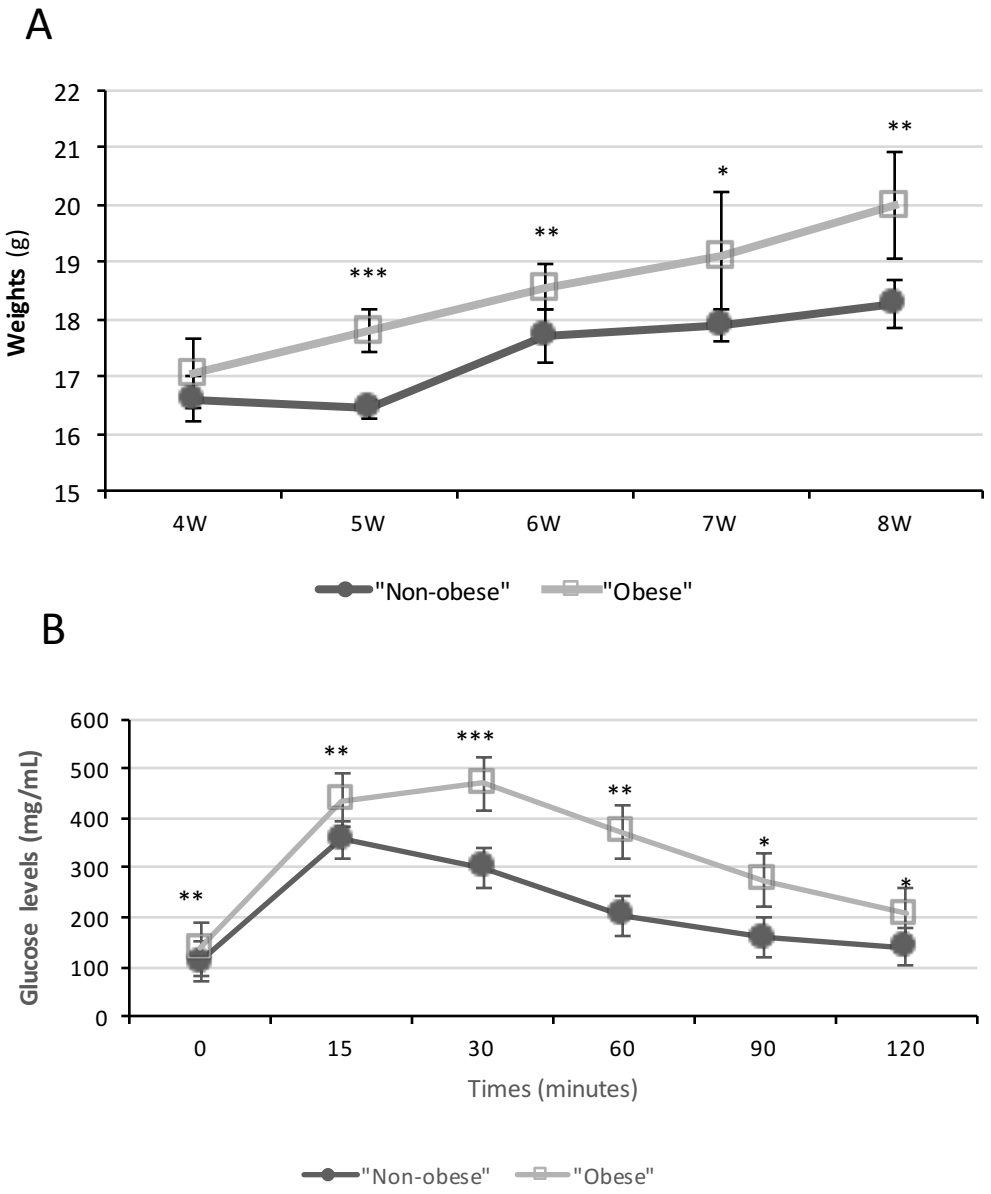

Supplementary Figure 12.
(A) Body weight compared between “Non-obese” and “Obese” mice in different ages. Five mice were used in each group (*$P < 0.05$, **$P < 0.01$, ***$P < 0.005$. Error bars represent means ± SD).
(B) Intraperitoneal glucose tolerance between “Non-obese” and “Obese” mice. Five mice were used in each group (*$P < 0.05$, **$P < 0.01$, ***$P < 0.005$. Error bars represent means ± SD).

Supplementary Figure 13

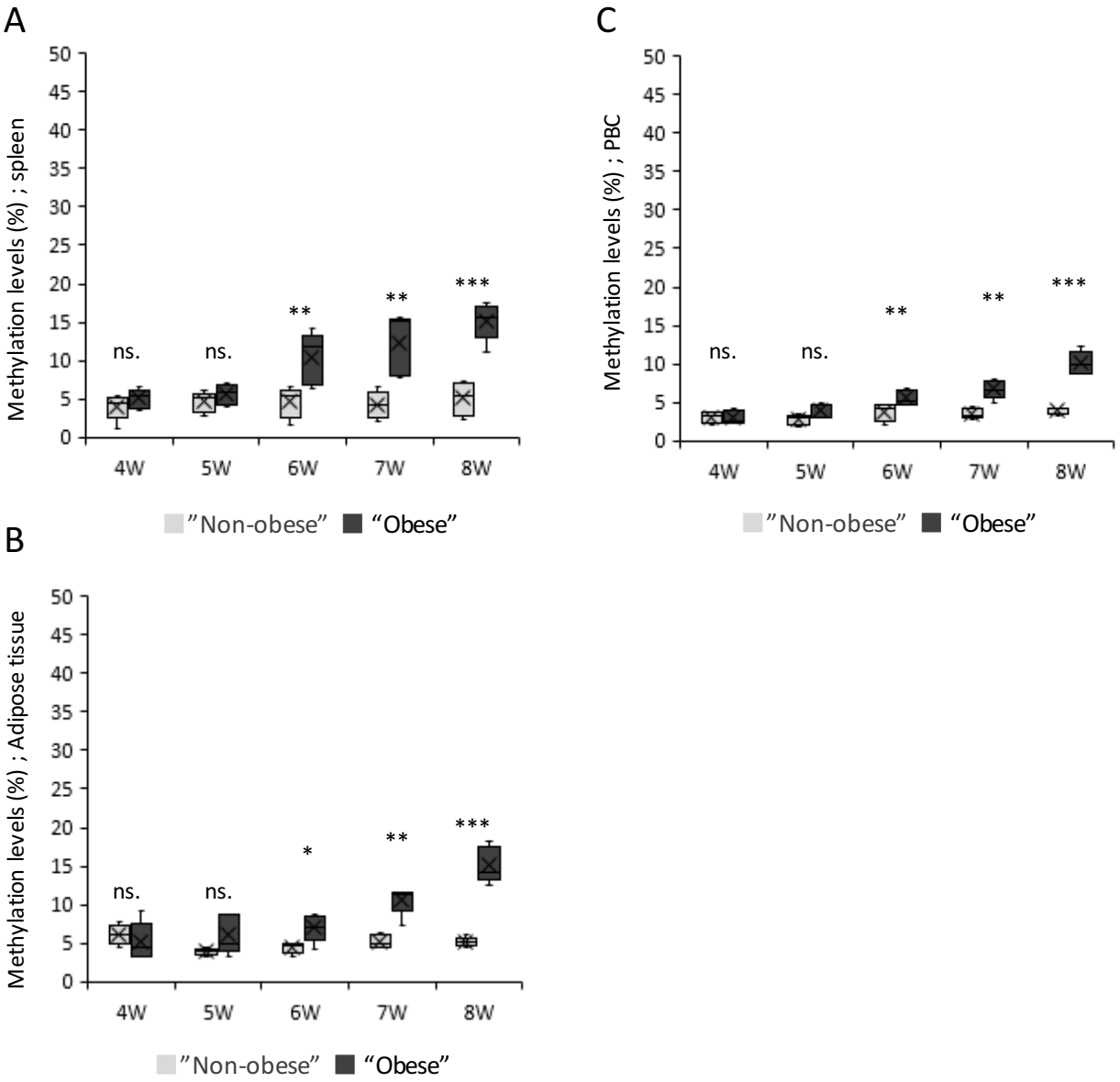

Supplementary Figure 13.
DNA methylation levels at P3 in *Klf14* compared between the “Obese” and “Non-obese” mice in the spleen (A), the adipose tissue (B) and PBC (C). Five mice were used in each group (*$P < 0.05$, **$P < 0.01$, ***$P < 0.005$. Error bars represent means ± SD).

Supplementary Figure 14

A

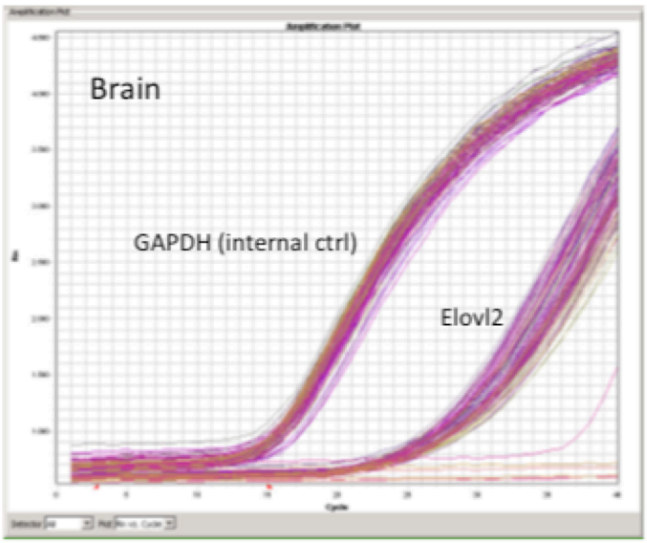

B

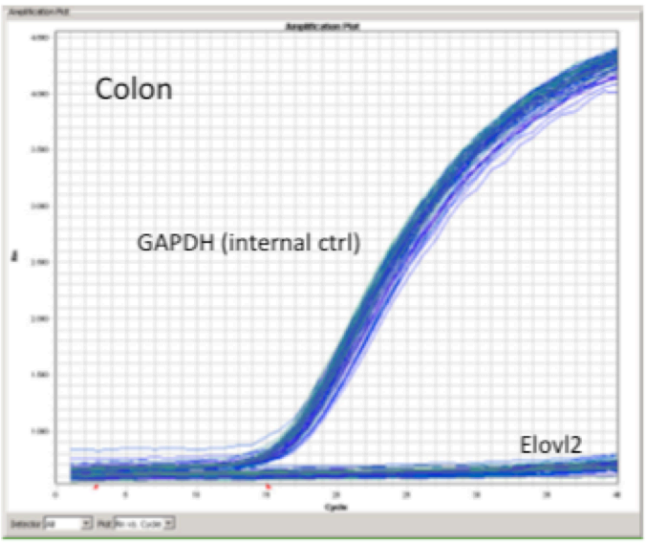

Supplementary Figure 14.
Amplification plot of *Elovl2* and *GAPDH* as an internal control. While *Elovl2* was detected in the brain (A), it was not detected in the colon (B),

Supplementary Figure 15

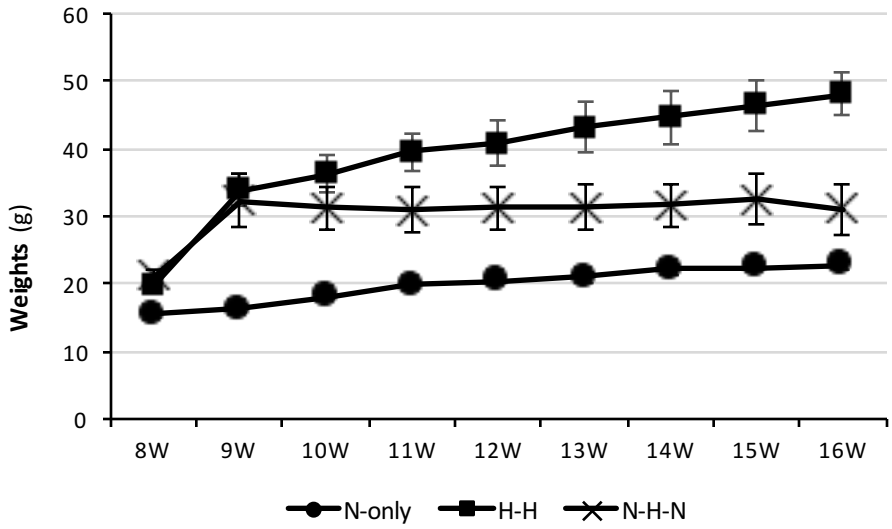

Supplementary Figure 15.
Body weight compared among “N-only”, “N-H” and “N-H-N” mice in different ages. Five mice were used in each group (*P < 0.05, **P < 0.01, ***P < 0.005. Error bars represent means ± SD).